

Dear Author,

Here are the proofs of your article.

- You can submit your corrections **online**, via **e-mail** or by **fax**.
- For **online** submission please insert your corrections in the online correction form. Always indicate the line number to which the correction refers.
- You can also insert your corrections in the proof PDF and **email** the annotated PDF.
- For fax submission, please ensure that your corrections are clearly legible. Use a fine black pen and write the correction in the margin, not too close to the edge of the page.
- Remember to note the **journal title**, **article number**, and **your name** when sending your response via e-mail or fax.
- **Check** the metadata sheet to make sure that the header information, especially author names and the corresponding affiliations are correctly shown.
- **Check** the questions that may have arisen during copy editing and insert your answers/ corrections.
- **Check** that the text is complete and that all figures, tables and their legends are included. Also check the accuracy of special characters, equations, and electronic supplementary material if applicable. If necessary refer to the *Edited manuscript*.
- The publication of inaccurate data such as dosages and units can have serious consequences. Please take particular care that all such details are correct.
- Please **do not** make changes that involve only matters of style. We have generally introduced forms that follow the journal's style. Substantial changes in content, e.g., new results, corrected values, title and authorship are not allowed without the approval of the responsible editor. In such a case, please contact the Editorial Office and return his/her consent together with the proof.
- If we do not receive your corrections **within 48 hours**, we will send you a reminder.
- Your article will be published **Online First** approximately one week after receipt of your corrected proofs. This is the **official first publication** citable with the DOI. **Further changes are, therefore, not possible.**
- The **printed version** will follow in a forthcoming issue.

Please note

After online publication, subscribers (personal/institutional) to this journal will have access to the complete article via the DOI using the URL: [http://dx.doi.org/\[DOI\]](http://dx.doi.org/[DOI]).

If you would like to know when your article has been published online, take advantage of our free alert service. For registration and further information go to: <http://www.springerlink.com>.

Due to the electronic nature of the procedure, the manuscript and the original figures will only be returned to you on special request. When you return your corrections, please inform us if you would like to have these documents returned.

Metadata of the article that will be visualized in OnlineFirst

ArticleTitle	Morphology and geology of the continental shelf and upper slope of southern Central Chile (33°S–43°S)	
Article Sub-Title		
Article CopyRight	Springer-Verlag (This will be the copyright line in the final PDF)	
Journal Name	International Journal of Earth Sciences	
Corresponding Author	Family Name	Völker
	Particle	
	Given Name	David
	Suffix	
	Division	
	Organization	Collaborative Research Center (SFB) 574 at the GEOMAR, Helmholtz Centre for Ocean Research Kiel
	Address	Wischhofstrasse 1-3, Kiel, 24148, Germany
	Email	dvoelker@geomar.de
Author	Family Name	Geersen
	Particle	
	Given Name	Jacob
	Suffix	
	Division	
	Organization	Collaborative Research Center (SFB) 574 at the GEOMAR, Helmholtz Centre for Ocean Research Kiel
	Address	Wischhofstrasse 1-3, Kiel, 24148, Germany
	Email	jgeersen@geomar.de
Author	Family Name	Contreras-Reyes
	Particle	
	Given Name	Eduardo
	Suffix	
	Division	Departamento de Geofísica
	Organization	Universidad de Chile
	Address	Santiago, Chile
	Email	econtreras@dgf.uchile.cl
Author	Family Name	Sellanes
	Particle	
	Given Name	Javier
	Suffix	
	Division	Departamento de Biología Marina
	Organization	Universidad Católica del Norte
	Address	Coquimbo, Chile
	Email	sellanes@ucn.cl
Author	Family Name	Pantoja
	Particle	
	Given Name	Silvio

	Suffix	
	Division	Departamento de Oceanografía y Centro de Investigación Oceanográfica en el Pacífico Sur-Oriental
	Organization	Universidad de Concepción
	Address	Concepción, Chile
	Email	spantoja@udec.cl
Author	Family Name	Rabbel
	Particle	
	Given Name	Wolfgang
	Suffix	
	Division	SFB574
	Organization	University of Kiel
	Address	Kiel, Germany
	Email	wrabbel@geophysik.uni-kiel.de
Author	Family Name	Thorwart
	Particle	
	Given Name	Martin
	Suffix	
	Division	
	Organization	University of Kiel
	Address	Kiel, Germany
	Email	thorwart@geophysik.uni-kiel.de
Author	Family Name	Reichert
	Particle	
	Given Name	Christian
	Suffix	
	Division	
	Organization	BGR Hannover
	Address	Hannover, Germany
	Email	Christian.Reichert@bgr.de
Author	Family Name	Block
	Particle	
	Given Name	Martin
	Suffix	
	Division	
	Organization	BGR Hannover
	Address	Hannover, Germany
	Email	Martin.Block@bgr.de
Author	Family Name	Weinrebe
	Particle	
	Given Name	Wilhelm Reimer
	Suffix	
	Division	
	Organization	Collaborative Research Center (SFB) 574 at the GEOMAR, Helmholtz Centre for Ocean Research Kiel
	Address	Wischofstrasse 1-3, Kiel, 24148, Germany

Email	wweinrebe@geomar.de
-------	---------------------

Schedule	Received	14 October 2011
	Revised	
	Accepted	21 May 2012

Abstract The continental shelf and slope of southern Central Chile have been subject to a number of international as well as Chilean research campaigns over the last 30 years. This work summarizes the geologic setting of the southern Central Chilean Continental shelf (33°S–43°S) using recently published geophysical, seismological, sedimentological and bio-geochemical data. Additionally, unpublished data such as reflection seismic profiles, swath bathymetry and observations on biota that allow further insights into the evolution of this continental platform are integrated. The outcome is an overview of the current knowledge about the geology of the southern Central Chilean shelf and upper slope. We observe both patches of reduced as well as high recent sedimentation on the shelf and upper slope, due to local redistribution of fluvial input, mainly governed by bottom currents and submarine canyons and highly productive upwelling zones. Shelf basins show highly variable thickness of Oligocene-Quaternary sedimentary units that are dissected by the marine continuations of upper plate faults known from land. Seismic velocity studies indicate that a paleo-accretionary complex that is sandwiched between the present, relatively small active accretionary prism and the continental crust forms the bulk of the continental margin of southern Central Chile.

Keywords (separated by '-') Southern Central Chile - Bathymetry - Shelf sedimentation - Shelf basins - Submarine faults - Seismicity - Fluid seepage

Footnote Information

Journal: 531
Article: 795



Author Query Form

**Please ensure you fill out your response to the queries raised below
and return this form along with your corrections**

Dear Author

During the process of typesetting your article, the following queries have arisen. Please check your typeset proof carefully against the queries listed below and mark the necessary changes either directly on the proof/online grid or in the 'Author's response' area provided below

Query	Details required	Author's response
1.	Please check and confirm that the authors and their respective affiliations have been correctly identified and amend if necessary.	
2.	Linke et al. (2011) has been changed to Linke (2011) so that this citation matches the list.	
3.	Please provide volume number for the reference Berger et al. (1987).	
4.	Please provide volume number and page range for the reference Hoffmann (1975).	
5.	Please provide page range for the reference Pizarro et al. (2002).	
6.	Please provide volume number for the reference Wiedicke-Hombach (2002).	
7.	Flueh et al. (1995) has been changed to Flueh (1995) so that this citation matches the list.	
8.	Hebbeln et al. (2001) has been changed to Hebbeln (2001) so that this citation matches the list.	
9.	Wiedicke et al. (2002) has been changed to Wiedicke-Hombach (2002) so that this citation matches the list.	

10.	Reference Farías et al. (2008) is given in list but not cited in text. Please cite in text or delete from list.	
11.	References Farías et al. (2010), Jessen et al. (2010), Völker et al. (2011a,b) are cited in text but not provided in the reference list. Please provide references in the list or delete these citations.	
12.	Please update the references "Dzierma et al., Scholz et al." with year.	

2 **Morphology and geology of the continental shelf and upper slope**
3 **of southern Central Chile (33°S–43°S)**

4 **David Völker · Jacob Geersen · Eduardo Contreras-Reyes · Javier Sellanes ·**
5 **Silvio Pantoja · Wolfgang Rabbel · Martin Thorwart · Christian Reichert ·**
6 **Martin Block · Wilhelm Reimer Weinrebe**

7 Received: 14 October 2011 / Accepted: 21 May 2012
8 © Springer-Verlag 2012

9 **Abstract** The continental shelf and slope of southern
10 Central Chile have been subject to a number of interna-
11 tional as well as Chilean research campaigns over the last
12 30 years. This work summarizes the geologic setting of the
13 southern Central Chilean Continental shelf (33°S–43°S)
14 using recently published geophysical, seismological, sedi-
15 mentological and bio-geochemical data. Additionally,
16 unpublished data such as reflection seismic profiles, swath
17 bathymetry and observations on biota that allow further
18 insights into the evolution of this continental platform are
19 integrated. The outcome is an overview of the current
20 knowledge about the geology of the southern Central
21 Chilean shelf and upper slope. We observe both patches of
22 reduced as well as high recent sedimentation on the shelf
23 and upper slope, due to local redistribution of fluvial input,
24 mainly governed by bottom currents and submarine can-
25 yons and highly productive upwelling zones. Shelf basins

show highly variable thickness of Oligocene-Quaternary
sedimentary units that are dissected by the marine contin-
uations of upper plate faults known from land. Seismic
velocity studies indicate that a paleo-accretionary complex
that is sandwiched between the present, relatively small
active accretionary prism and the continental crust forms
the bulk of the continental margin of southern Central Chile.

Keywords Southern Central Chile · Bathymetry ·
Shelf sedimentation · Shelf basins · Submarine faults ·
Seismicity · Fluid seepage

Introduction 37

The southern Central Chilean continental margin has been
subject to geological and geophysical research for the last

A1 D. Völker (✉) · J. Geersen · W. R. Weinrebe
A2 Collaborative Research Center (SFB) 574 at the GEOMAR,
A3 Helmholtz Centre for Ocean Research Kiel,
A4 Wischhofstrasse 1-3, 24148 Kiel, Germany
A5 e-mail: dvoelker@geomar.de

A6 J. Geersen
A7 e-mail: jgeersen@geomar.de
A8 W. R. Weinrebe
A9 e-mail: wwainrebe@geomar.de

A10 E. Contreras-Reyes
A11 Departamento de Geofísica, Universidad de Chile,
A12 Santiago, Chile
A13 e-mail: econtreras@dgf.uchile.cl

A14 J. Sellanes
A15 Departamento de Biología Marina,
A16 Universidad Católica del Norte, Coquimbo, Chile
A17 e-mail: sellanes@ucn.cl

A18 S. Pantoja
A19 Departamento de Oceanografía y Centro de Investigación
A20 Oceanográfica en el Pacífico Sur-Oriental, Universidad
A21 de Concepción, Concepción, Chile
A22 e-mail: spantoja@udec.cl

A23 W. Rabbel
A24 SFB574, University of Kiel, Kiel, Germany
A25 e-mail: wrabbel@geophysik.uni-kiel.de

A26 M. Thorwart
A27 University of Kiel, Kiel, Germany
A28 e-mail: thorwart@geophysik.uni-kiel.de

A29 C. Reichert · M. Block
A30 BGR Hannover, Hannover, Germany
A31 e-mail: Christian.Reichert@bgr.de

A32 M. Block
A33 e-mail: Martin.Block@bgr.de

40 decades, resulting in a variety of different data sets from
 41 international and Chilean research cruises (Table 1). Some
 42 of the data are published in international peer-reviewed
 43 journals, but a number of data sets, and in particular those
 44 collected over recent years, remain yet unpublished. In
 45 addition, a few review articles and book chapters combine
 46 and summarize aspects of the conducted research, and
 47 especially the book “The Andes-Active Subduction Oro-
 48 geny” (Oncken et al. 2006) provides an important overview.
 49 However, no review article summarizes the geologic setting
 50 of the continental shelf and uppermost slope of southern
 51 Central Chile. Here, we tie together the current knowledge
 52 about the geology of that part of the Chilean Shelf that has
 53 the best data coverage (between 33°S and 43°S) by
 54 reviewing previously published data sets and expand this
 55 knowledge by adding previously unpublished seismic
 56 reflection, bathymetric, seismological and biological data as
 57 well as data sets that were published in cruise reports and
 58 doctoral theses. The new data include (1) today’s most
 59 comprehensive bathymetric data which we produced from
 60 swath bathymetric data of eight scientific cruises (Weinrebe
 61 et al. 2011) merged with a bathymetric data set of Zapata
 62 (2001); (2) unpublished sediment-echosounder data from
 63 the continental slope; (3) an unpublished seismic reflection
 64 line that runs N–S from 36.75°S to 40°S (SO161-25). The
 65 information that is assembled in this work covers the region
 66 with a highly variable density. While we provide seismic
 67 insights into some forearc basins (Arauco and Valdivia
 68 Basin, Fig. 1), we lack similar data of neighbouring basins.
 69 In total, there is still a lack of data for the comprehensive
 70 understanding of the continental shelf, such as of bathy-
 71 metric mapping campaigns of the shelf, margin-parallel
 72 seismic reflection profile studies, drilling transects and
 73 bottom current measurements.

74 Geologic and tectonic framework of the southern 75 Central Chilean continental margin

76 The convergent continental margin of southern Central
 77 Chile between 33°S and 43°S is characterized by a trench
 78 that is filled by up to 2.5 km of sediment. This sediment-
 79 filled part of the Peru–Chile Trench is limited by two
 80 elevated topographic features of the oceanic crust, the Juan
 81 Fernández Ridge that enters the subduction zone at 32°S
 82 and the Chile Ridge that subducts at the Chile Triple
 83 Junction at around 46°S (Fig. 1). The main structural
 84 elements across the marine part of the continental margin
 85 are the 40–80 km wide Peru–Chile Trench Basin, a young
 86 (late Pliocene–Pleistocene) frontal accretionary prism at
 87 the lower slope that is 5–40 km wide (Bangs and Cande
 88 1997; Contreras-Reyes et al. 2010; Geersen et al. 2011a), a
 89 relatively smooth upper continental slope with sedimentary
 90 slope basins, thrust ridges, deeply incised submarine

canyon systems and mass-wasting features and a conti-
 91 nental shelf that is dissected by submarine canyons and
 92 partly shaped by mass-wasting features (Fig. 1; detailed
 93 maps Figures 2–6).
 94

The tectonic framework of the southern Central Chilean
 95 continental margin is controlled by the subduction of the
 96 oceanic Nazca Plate underneath the South American Plate
 97 (Fig. 1). The Nazca Plate subducts obliquely with an angle
 98 of 80.1° at a rate of 66 mm/a (Angermann et al. 1999). The
 99 subduction rate has varied in the past and decreased
 100 ~40 % over the last 20 Ma (Somoza 1998; Oncken et al.
 101 2006). The volume of the 5–40 km wide accretionary
 102 prism is not compatible with a continuous history of
 103 accretion over time periods of tens of millions of years,
 104 which implies episodic phases of tectonic accretion, non-
 105 accretion and erosion (Bangs and Cande 1997). Melnick
 106 and Echtler (2006a) argued that during Pliocene the margin
 107 shifted from erosive to accretionary mode in response to an
 108 increase in trench sedimentation rate, linked to fast denu-
 109 dation of the Andes and a coeval decrease of the subduc-
 110 tion rate. Similarly, Kukowski and Oncken (2006)
 111 suggested that the southern Central Chile subduction zone
 112 has been in accretion mode since the Pliocene, following
 113 on a period of subduction erosion that started at least in the
 114 middle Miocene. The subduction process impacts on the
 115 evolution of the shelf and upper slope of southern Central
 116 Chile in a number of ways:
 117

1. The subduction of submarine ridges, seamounts and
 118 thickened crust has led to mass removal and local
 119 subsidence of the marine forearc, for example at 33°S
 120 where the subduction of the Juan Fernández Ridge is
 121 taking place. This process created accommodation
 122 space for marine forearc basins on the upper conti-
 123 nental slope that form important depocentres for
 124 sediments close to the continental shelf (von Huene
 125 et al. 1997; Laursen et al. 2002).
 126
2. Basal accretion of underthrust trench sediments has
 127 been made responsible for focused and localized uplift
 128 of coast and shelf segments in particular off Arauco
 129 Peninsula (Lohrmann et al. 2006). Here, ~1.5 km of
 130 uplift during Middle Pliocene has been reported
 131 (Melnick and Echtler 2006a; Melnick et al. 2006).
 132
3. Oblique subduction of the Nazca Plate is responsible
 133 for the development of a forearc sliver, the Chiloé
 134 Microplate, that extends from the Chile Triple Junction
 135 at ~46°S to the Arauco Peninsula at ~38°S (Melnick
 136 et al. 2009). The Chiloé Microplate is decoupled from
 137 the stable South American Plate along the Liquiñe-
 138 Ofqui Fault Zone (LOFZ, Fig. 1), a prominent margin-
 139 parallel fault system that has been active in a
 140 transpressional dextral motion since the Pliocene
 141 (Cembrano et al. 2000; Rosenau 2004; Rosenau et al.
 142

Table 1 Meta-information on cruises of German vessels SONNE and METEOR as well as raw bathymetric data sets are stored at the Bundesamt für Seeschifffahrt und Hydrographie (BSH) at <http://www.bsh.de>

Inventory of scientific cruises and geophysical data offshore southern Central Chile					
Ruise/ship expedition	Method	Data	Latitudes	Partly published in	Cruise reports or chief scientist
RV SONNE SO101-102	Swath bathymetry	Along track	21°S–44°S	von Huene et al. (1997), this study	Hebbeln and Wefer (1995)
	Sediment echosounder	Along track			
	Reflection seismics	37 profiles			
RV SONNE SO103	Multicores	42 cores	31.5°S–34°S	Flueh et al. (1998)	Flueh (1995)
	Gravity cores	63 cores		Laursen et al. (2002)	
	Swath bathymetry	Along track		Laursen and Normark (2003)	
	Sediment echosounder	Along track		Lamy et al. (1998, 2001)	
	Swath bathymetry	Along track		Hebbeln et al. (2000)	
RV SONNE SO104	Sediment echosounder	Along track	20°S–32°S	Lamy et al. (1999)	R. von Huene
	Swath bathymetry	Along track		This study	
	Sediment echosounder	Along track		Laursen and Normark (2002), this study	
	Reflection seismics	14 profiles		von Huene et al. (1997)	
RV SONNE SO156	Swath bathymetry	Along track	22°S–44°S	Laursen et al. (2002)	Hebbeln (2001)
	Sediment echosounder	Along track		Laursen and Normark (2002)	
	Multicores	163 cores		Ranero et al. (2006)	
	Swath bathymetry	Along track		This study	
	Sediment echosounder	Along track		Muñoz et al. (2004)	
RV SONNE SO161	Gravity cores	91 cores	23°S–38°S	Stuut et al. (2007)	Reichert (2002) Flueh et al. (2002) Wiedicke-Hombach (2002)
	Swath bathymetry	Along track		This study	
	Sediment echosounder	Along track		This study	
	Reflection seismics	35 profiles		Rauch (2005)	
	Swath bathymetry	Along track		Ranero et al. (2006)	
RV SONNE SO161	Sediment echosounder	Along track	23°S–38°S	Völker et al. (2006)	Wiedicke-Hombach (2002)
	Reflection seismics	35 profiles		Contreras-Reyes et al. (2008)	
	Swath bathymetry	Along track		Rodrigo et al. (2009)	
RV SONNE SO161	Gravity cores	29 cores	23°S–38°S	Geersen et al. (2011b)	Wiedicke-Hombach (2002)
	Swath bathymetry	Along track		Völker et al. (2008)	
RV SONNE SO161	Gravity cores	29 cores	23°S–38°S	Blumberg et al. (2008)	Wiedicke-Hombach (2002)
	Swath bathymetry	Along track		Blumberg et al. (2008)	

Table 1 continued

Inventory of scientific cruises and geophysical data offshore southern Central Chile

Ruise/ship expedition	Method	Data	Latitudes	Partly published in	Cruise reports or chief scientist
RV SONNE SO181	Swath bathymetry Sediment echosounder Reflection seismics	Along track Along track 4 profiles	31°S–47°S	This study	Flueh and Grevemeyer (2005)
RV SONNE SO210	Gravity cores Swath bathymetry	16 cores Along track	33°S–38.5°S	Contreras-Reyes et al. (2008, 2010) Scherwath et al. (2009) Heberer et al. (2010) Völker et al. (2012) Völker et al. (2011), this study	Linke (2011)
RRS James Cook JC23	Sediment echosounder Gravity cores Swath bathymetry	Along track 14 cores Along track	33°S–38°S	This study This study Völker et al. (2011a), this study Geersen et al. (2009) Völker et al. (2009) Klaucke et al. (2012) Moscoso et al. (2011) Bangs and Cande (1997) Díaz-Naveas (1999) Contreras-Reyes et al. (2008) Scherwath et al. (2009) Geersen et al. (2011a) Fossing et al. (1995) Lamy (1998) Hebbeln et al. (2000)	Flueh and Bialas (2008)
R/V CONRAD 2901	Gravity cores Sidescan sonar Wide-angle seismic Reflection seismics	13 cores 4 profiles 4 profiles 6 profiles	32°S–40°S		
R/V VIDAL GORMAZ 1994 (Thioplaca)	Multicores	5 cores			
R/V VIDAL GORMAZ VG02	Swath bathymetry Reflection seismics	Along track 18 profiles	31°S–34°S	This study	J. Díaz-Naveas
R/V VIDAL GORMAZ VG06	Swath bathymetry Reflection seismics	Along track	32.5°S–37°S	Contardo et al. (2008) Contardo et al. (2008)	J. Díaz-Naveas
RV METEOR M67	Swath bathymetry Sediment echosounder Gravity cores	Along track Along track 8 gravity cores	33°S–37°S	This study	Weinrebe and Schenk (2006)
RV MELVILLE MV1004 ODP leg 202	Swath bathymetry Drill cores	Along track ODP sites 1233, 1234, 1235	34°S–38°S 35°S–40°S	Blumberg et al. (2008)	C. D. Chadwell Mix et al. (2003)

Metadata on cruises of US research vessels are stored at the Geological Data Center of the Scripps Institute of Oceanography: <http://gdc.ucsd.edu/>

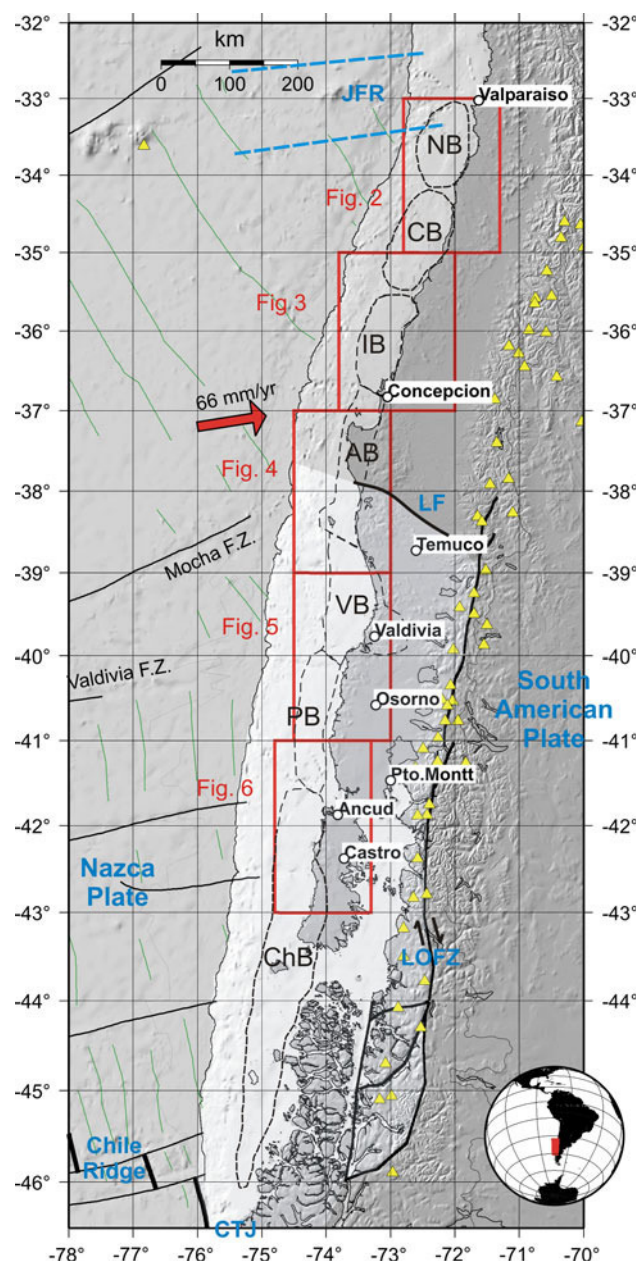


Fig. 1 Overview map of southern Central Chile with main tectonic units. Boxes indicate the positions of Figures 2–6. The lighter shaded area corresponds to the outline of the Chilóe Microplate (Melnick et al. 2009). The position of shelf basins (stippled lines) is according to Melnick and Echtler (2006b). Yellow triangles are Quaternary volcanoes of the Southern Volcanic Zone (Siebert and Simkin 2002). LOFZ Liquiñe-Ofqui Fault Zone, LF Lanahue Fault, JFR Juan Fernández Ridge, CTJ Chile triple junction, NB Navidad Basin, CB Chanco Basin, IB Itata Basin, AB Arauco Basin, VB Valdivia Basin, PB Pucatrihue Basin, ChB Chilóe Basin

148
149
150
151
152

2006; Thomson 2002). The collision of the Chilóe Microplate that moves northward at a present rate of 6.5 mm/a (Wang et al. 2007) with the South American Plate in the region of the Arauco Peninsula is a likely cause for the existence of a number of SE-NW trending

upper plate faults that are mapped in the terrestrial forearc (Melnick and Echtler 2006b; Melnick et al. 2009). Active shortening across such faults caused the orogenesis of the Nahuelbuta Coastal Range (Melnick et al. 2009). An indirect consequence of the differential uplift is the shift and reorganization of river networks on land and their respective submarine continuations (canyon systems) that cut deeply into the shelf and continental slope (Rehak et al. 2008).

4. The Chilean subduction zone produces powerful megathrust earthquakes of $M_w > 8$ almost in decadal intervals (e.g. Bilek 2010), and the historic record shows that these recur in spatially defined seismotectonic segments of the forearc (Lomnitz 2004). In the study area, the M_w 9.5 Great Chile Earthquake of 22 May 1960 and the M_w 8.8 Maule Earthquake of 27 February 2010 stand out as the largest and sixth largest ever instrumentally recorded earthquakes in the world. The earthquakes have historical recurrence times of 100–200 years per segment and cause coseismic horizontal motions of some 10 m and vertical motions of some metres of the coastal areas and the shelf (Cifuentes 1989; Barrientos and Ward 1990; Cisternas et al. 2005; Moreno et al. 2009; Farías et al. 2010). Megathrust earthquakes were historically and recently associated with tsunamis that devastated coastal areas and deposited specific tsunami deposits in estuaries (Cisternas et al. 2005; Vargas et al. 2011).

153
154
155
156
157
158
159
160
161
162
163
164
165
166
167
168
169
170
171
172
173
174
175
176
177
178
179
180

Climate

181

The denudation rate of the Andes shows a distinct climatic component related to Hadley cell-driven precipitation regimes (Montgomery et al. 2001). The central part of the range (15°S–33°S) is in the subtropical belt of deserts, where there is little precipitation on either side of the range. To the south, Westerlies bring abundant moisture that precipitates at the western slopes of the Andes, resulting in a significant increase in the mean annual precipitation rate from <0.5 m/y at around 30°S to 2–3 m/y south of 38°S (Hoffmann 1975) and a mean annual river run-off of 0.25–0.5 mm/y (Fekete et al. 2000). In the vicinity of the Chile Triple Junction (46°S), apatite fission track ages from the western flank of the Andes imply that 3–4 km of denudation occurred in this region since ~17 Ma (Haschke et al. 2006).

Oceanographic features

197
198
199
200

The poleward Gunther Undercurrent (or Poleward Undercurrent) at 0.2–0.5 km water depth flows close enough to the edge of the shelf to induce coast-parallel southward

201 sediment transport. Current velocities from 0.1 to 0.5 m/s
 202 at depths of 100–300 m were measured (Huyer et al. 1991;
 203 Pizarro et al. 2002). Shaffer et al. (1995, 1997, 1999)
 204 reported a mean value of 0.128 m/s and a maximum value
 205 of 0.689 m/s over a period of 6 years.

206 The coasts of Valparaíso and Concepción are well
 207 known zones of intense coastal upwelling (e.g. Djurfeldt
 208 1989; Figueroa and Moffat 2000). These conditions lead to
 209 extremely high biogenic productivity (Daneri et al. 2000;
 210 Atkinson et al. 2002) and carbon fixation resulting in
 211 annual production rates of $>200 \text{ g C/m}^2$ (Berger et al.
 212 1987) which has a pronounced impact on the slope sedi-
 213 mentation (Hebbeln et al. 2000). South of 38°S, prevailing
 214 onshore winds of the Westerlies generally prevent coastal
 215 upwelling (Strub et al. 1998), but nonetheless areas of high
 216 primary productivity exist south of 40°S. Hebbeln et al.
 217 (2000) propose either advection of the Antarctic Circum-
 218 polar Current and/or river input as nutrient sources that
 219 sustain this effect. Tidal currents can have a strong effect
 220 on local deposition as they are very strong at the outlets of
 221 estuaries and in particular at the outlet of the Gulf of
 222 Ancud, the Chacao Channel ($\sim 4 \text{ m/s}$, Cáceres et al. 2003,
 223 Fig. 6).

224 Sediment input

225 The main source area for sediments deposited at the
 226 southern Central Chile continental margin is the western
 227 flank of the Andean Cordillera. Sediments are brought to
 228 the Pacific Ocean mainly by river systems (Lamy et al.
 229 1998, 1999) that emerge from the Andean Cordillera, cross
 230 the Central Valley of Chile and the Coastal Cordillera and
 231 partly continue in submarine canyon systems. A fraction of
 232 the clastic material eroded from the Andes forms the fill of
 233 the Central Valley, another fraction is deposited in sedi-
 234 mentary basins of the submarine forearc and the open slope
 235 or is temporarily stored in the submarine canyons (Raitzsch
 236 et al. 2007). A second source of sediments is the Coastal
 237 Cordillera that reaches elevations of 2,200 m in the Val-
 238 paraíso region (33°S) and almost 1,600 m in the Cordillera
 239 de Nahuelbuta ($\sim 37.5^\circ\text{S}$, Fig. 4). Strong precipitation and
 240 high river discharge transport huge amounts of terrigenous
 241 matter to the ocean between 35° and 39°S (suspended
 242 particles = 600–2,500 ton per month; <http://www.dga.cl>;
 243 Muñoz et al. 2004).

244 The Southern Volcanic Zone (SVZ) of the Andes (33°S–
 245 46°S) is associated with the Nazca Plate subduction
 246 (López-Escobar et al. 1993). The SVZ includes at least 60
 247 historically and potentially active volcanic edifices in Chile
 248 and Argentina, three giant silicic caldera systems (Maipo,
 249 Calabozos and Caviahué) and numerous minor eruptive
 250 centres (Siebert and Simkin 2002; Stern 2004; Stern et al.
 251 2007). Explosive volcanism has led to the deposition of

252 ash fallout deposits in prehistoric and historic eruptions
 253 (e.g. Hildreth et al. 1984; Haberle and Lumley 1998;
 254 Naranjo and Stern 1998, 2004; Hildreth and Drake 1992;
 255 Sruoga et al. 2005), and the tephra layers are widespread
 256 over Chile and Argentina. A fraction of this volcanic ash
 257 has been deposited offshore (ODP leg 202 sites 1233,
 258 1234,1235, Mix et al. 2003; Völker et al. 2006, 2009; Linke
 259 2011).

260 The third major source of sediment particles is the
 261 biogenic production related to the coastal upwelling
 262 zones. Biogenic constituents vary in abundance and consist
 263 primarily of nannofossils and diatoms with less abundant
 264 silicoflagellates and foraminifers in general (Mix et al.
 265 2003). Variations in the abundance and species composi-
 266 tion of foraminifera are related to water productivity and
 267 regional variations of upwelling (Hebbeln et al. 2000).
 268 Patches of authigenic carbonates are observed at the sea-
 269 floor in areas where methane seepage is reported (Linke
 270 2011). The microbial process of anaerobic oxidation of
 271 methane is, however, mainly restricted to the Oxygen
 272 Minimum Zone below $\sim 800 \text{ m}$ water depth and is related
 273 to the high productivity areas of coastal upwelling (Treude
 274 et al. 2005).

Morphology of the continental shelf and upper slope 275

276 The morphological information described here and pre-
 277 sented in Figs. 2, 3, 4, 5, 6 is the result of joining swath
 278 bathymetry data that were recorded on 12 cruises of
 279 research vessels SONNE, METEOR, VIDAL GORMAZ
 280 and JAMES COOK between 1995 and December 2010
 281 (Table 1) and that mainly cover the continental slope with a
 282 gridded Chilean data set of the shelf morphology (Zapata
 283 2001). The swath bathymetry data, in total more than 8,000
 284 data files comprising about 1.1 billion soundings, were
 285 recorded with different swath bathymetry systems, but
 286 mostly with the Kongsberg EM-120 system. We processed
 287 the raw data using the MB-Systems software (Caress et al.
 288 1996). Processing steps comprised the check of navigation
 289 data, interpolation of missing navigation values, calculation
 290 of water depth and positions of the footprints of the beams
 291 by ray tracing through the water column and removal of
 292 artefacts and erroneous data points. Processed data of the
 293 bathymetric systems were then combined into digital ele-
 294 vation models (DEMs) with a grid point density of 200 m.
 295 Then, we merged the grids with a clipped version of the
 296 gridded bathymetry data of Zapata (2001). The Zapata data
 297 set has a lower grid point density of about 800 m and lacks
 298 many details that show up in the raw bathymetry data, but as
 299 those seldom cover the shelf we use the Zapata data set as
 300 background information. We clipped the Zapata data to the
 301 water depth range of 0–400 m and included them to the grid

302 calculation with a low weighting factor for the splines
 303 calculation of new grid points. The resulting grid is satisfac-
 304 tory for most of the shelf and slope areas, and however in
 305 some places, the interpolation between the high-density raw
 306 and low-density gridded data produces artefacts which we
 307 had to remove manually. Finally, the grids were combined
 308 with the land topography data of the Shuttle Radar
 309 Topography Mission (SRTM; Farr 2007).

310 Between 33°S and 43°S, the continental shelf is rela-
 311 tively narrow with a mean width of 30–40 km (Figs. 2, 3,
 312 4, 5, 6). The width of the shelf from the coast to the shelf
 313 break at ~200 m water depth is narrower offshore prom-
 314 inent promontories as well as where the Coastal Cordillera
 315 is close to the coast such as offshore Valparaíso (33°S)
 316 and Pichilemu (34.5°S) (width 20 km), while coastal

317 embayments such as the Golfo de Arauco (37°S) form
 318 regions of a wider continental platform (width 40 km). The
 319 maximum width is offshore Arauco Peninsula at Mocha
 320 Island and offshore Chiloé Island (~60 km).

321 At 41.8°S, the N–S trending coastline is interrupted by
 322 the Canal de Chacao that separates Chiloé Island from the
 323 mainland (Fig. 6). As the continental forearc subsides to
 324 the south, the Coastal Cordillera continues as the back-
 325 bone of Chiloé Island, whereas the southward continua-
 326 tion of the Chilean Central Valley is drowned to form the
 327 shallow (<250 m) Golfo Corcovado and Golfo de Ancud
 328 between the mainland and Chiloé Island. This 45-km-
 329 wide (E–W) and 90-km-long (N–S) gulf is a semi-
 330 enclosed marine forearc basin in the back of Chiloé Island
 331 that is protected from the direct Pacific swell and unique

Fig. 2 Bathymetric map of the Chilean shelf and upper slope from 33°S to 35°S. *Blue circles* denote epicentres of aftershocks of the Feb 27, 2010, Mw 8.8 Maule earthquake (Servicio Sismológico Line 444: Either “of Jurassic age and” or “inner prism, presumably of Jurassic age, represents” de Chile, ssn.dgf.uchile.cl, time window of 27.02.2010–13.04.2010). The Pichilemu seismic sequence of the 11.03.2010 (Fariás et al. 2011) is highlighted by *yellow fill*. *Square symbols* indicate sediment samples described by Hebbeln et al. (2000) and Lamy et al. (1998). *Stippled black lines* correspond to outlines of shelf basins. Bathymetric information is composed of a data set of a number of RV SONNE cruises, RRS JAMES COOK cruise JC23 and a shallow-water data set compiled by Zapata (2001). Land topography was extracted from the SRTM data set (Farr et al. 2007), absence of bathymetric information is indicated as *grey areas*. Slope canyon names are in *yellow boxes*

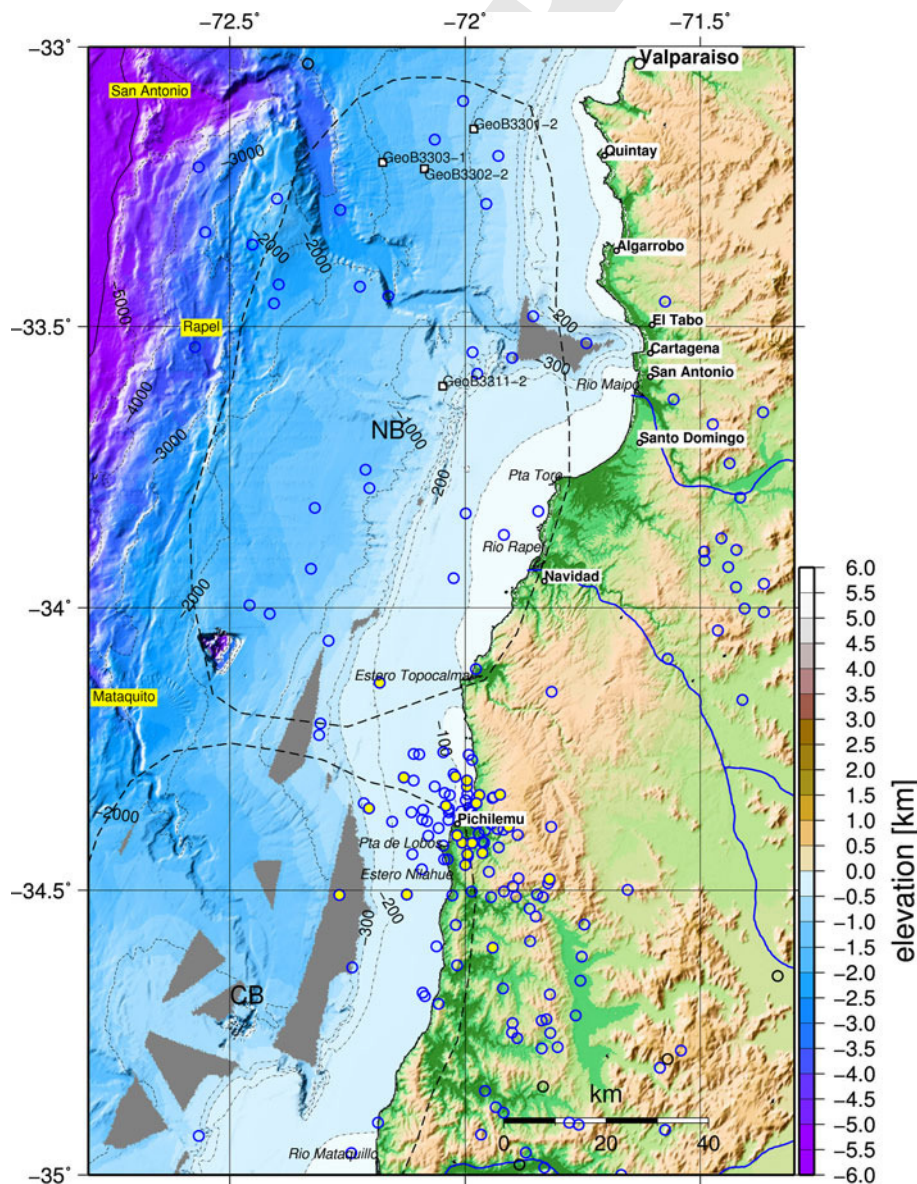
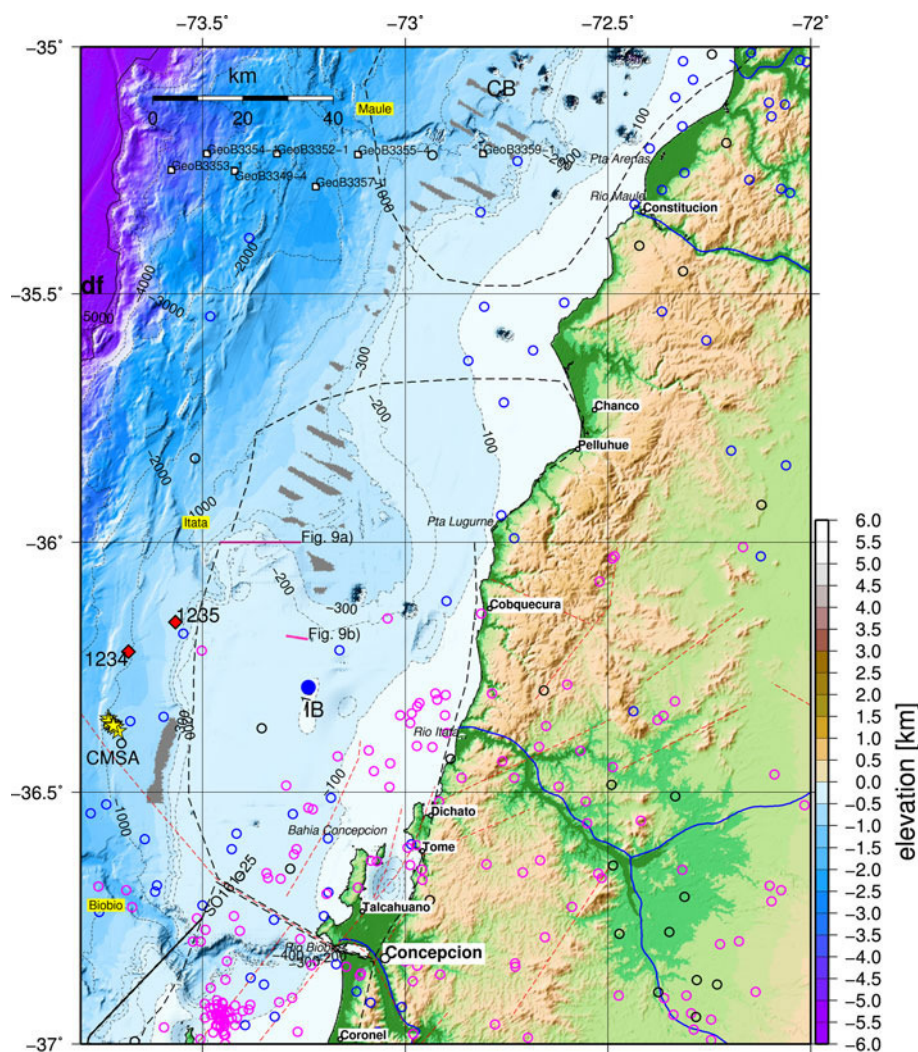


Fig. 3 Bathymetric map of the Chilean shelf and upper slope from 35°S to 37°S (Maule Province). *Black lines* indicate the position of seismic profiles of the SPOC project shot on RV SONNE cruise SO161 (Reichert 2002). *Pink lines* indicate PARASOUND sediment-echosounder profiles that are referred to in the text. *Circles* denote epicentres of main and aftershocks of the Maule earthquake (Servicio Sismológico de Chile, ssn.dgf.uchile.cl, time window of 27.02.2010–13.04.2010 *blue*, main shock: *blue filled*) and of Bohm et al. 2002 (*magenta*). *Red diamonds* indicate ODP leg 202 drill sites. *Square symbols* indicate sediment samples described by Hebbeln et al. (2000) and Lamy et al. (1998). *CMSA* concepción methane seepage area. *Yellow stars* show observations of biocommunities related to gas seepage (Sellanes et al. 2004; Sellanes and Krylova 2005). *Stippled black lines* correspond to outlines of shelf basins. Absence of bathymetric information is indicated as *grey areas*



332 for Chile in this respect. With the subsidence of the
333 Central Valley to below sea level, the coastline south of
334 42°S directly touches the Central Cordillera of the Andes
335 and forms a fjord coast.

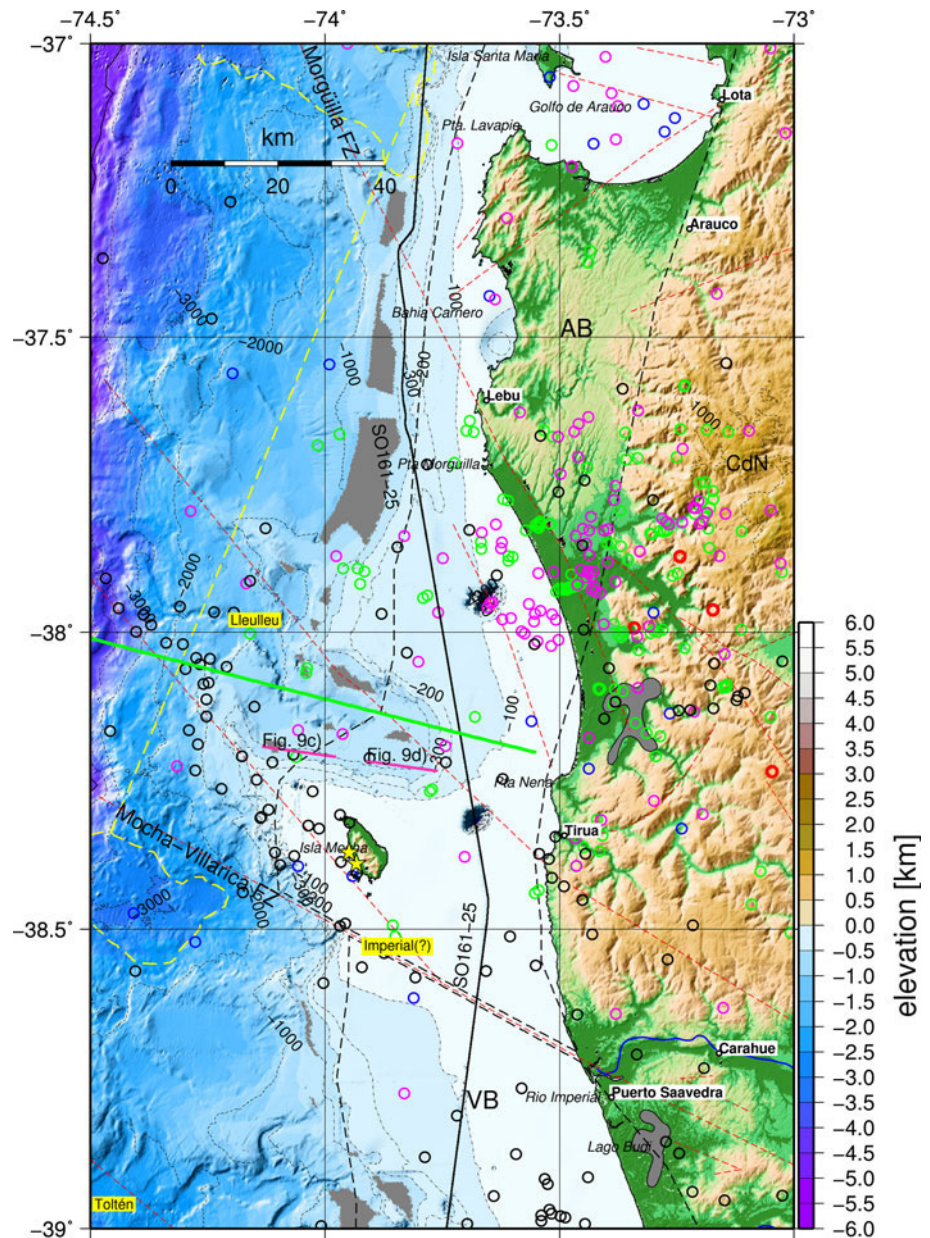
336 The shelf edge lies at a water depth range of 150–300 m.
337 It is well defined where the shelf is wider such as offshore
338 the Golfo de Arauco (37°S, Fig. 4), west of Mocha Island
339 (38.2°S Fig. 4) and offshore Chiloé Island. Offshore
340 Arauco Peninsula, the shelf edge is at some places indented
341 by headscarps of ancient giant slope failures (Geersen et al.
342 2011b).

343 The upper continental slope shows a relatively smooth
344 morphology and is inclined at low angles (2–4°) to a water
345 depth of 2,000 m. Below 2,000 m water depth, the slope
346 morphology is less regular with steep slope segments (up to
347 30°) alternating with roughly trench-parallel belts of less
348 steep and even landward verging seafloor. This irregular
349 morphology is caused by the continuous deformation of the
350 ~4 Ma young accretionary prism that forms the lower
351 continental slope.

Submarine canyon systems

352
353 A number of submarine canyons dissect the continental
354 slope and partly cut into the shelf to connect directly
355 to feeding river systems. We use the nomenclature of Rodrigo
356 (2010). From north to south, the submarine canyons are (1)
357 San Antonio Canyon, connected to the mouth of Río Maipo
358 (Hagen et al. 1996; Laursen and Normark 2002, Fig. 2); (2)
359 Rapel Canyon; (3) Mataquito Canyon between 34°S and
360 34.7°S that is possibly linked to Río Mataquillo/Mataquito
361 (Fig. 2); (4) Maule Canyon, connected to Río Maule
362 (Fig. 3); (5) Itata Canyon, connected to Río Itata (Fig. 3);
363 (6) the prominent BíoBío Canyon (with its major confluence
364 Santa Maria Canyon) that cuts deep into the shelf and
365 forms a direct continuation of the BioBío River (Fig. 3);
366 (7) Lleulleu Canyon (or Paleo-Pellahuen Canyon) directly
367 north of Mocha Island once formed the marine continua-
368 tion of Pellahuen River before the latter was deflected due
369 to uplift of Arauco Peninsula according to Rehak et al.
370 (2008, Fig. 4); (8) Imperial Canyon is a canyon that is

Fig. 4 Bathymetric map of the Chilean shelf and upper slope from 37°S to 39°S (Arauco Peninsula). *Black lines* indicate the position of seismic profiles of the SPOC project shot on RV SONNE cruise SO161 (Reichert 2002). *Pink lines* indicate PARASOUND sediment-echosounder profiles that are referred to in the text. *Yellow stippled lines* denote headwall and sidewalls of giant slope failures of Geersen et al. (2011b). *Circles* denote epicentres (*blue*: main and aftershocks of the Maule earthquake, Servicio Sismológico de Chile, ssn.dgf.uchile.cl/, *magenta*: Bohm et al. 2002, *red*: main and aftershocks of the 1960 earthquake, Engdahl and Villaseñor 2002 in the time window of 21.05–25.05.1960, *green*: Haberland et al. 2006, *black*: Dzierma et al. submitted). *Yellow stars* show observations of gas seepage at Mocha Island (Jessen et al. 2010). The wide-angle seismic profile of Contreras-Reyes et al. (2008) is depicted as *green line*. *Red stippled lines* show tectonic faults mapped on land between 36°S and 42°S by Melnick and Echter (2006b). *CdN* Cordillera de Nahuelbuta. *Stippled black lines* correspond to outlines of shelf basins. Absence of bathymetric information is indicated as *grey areas*

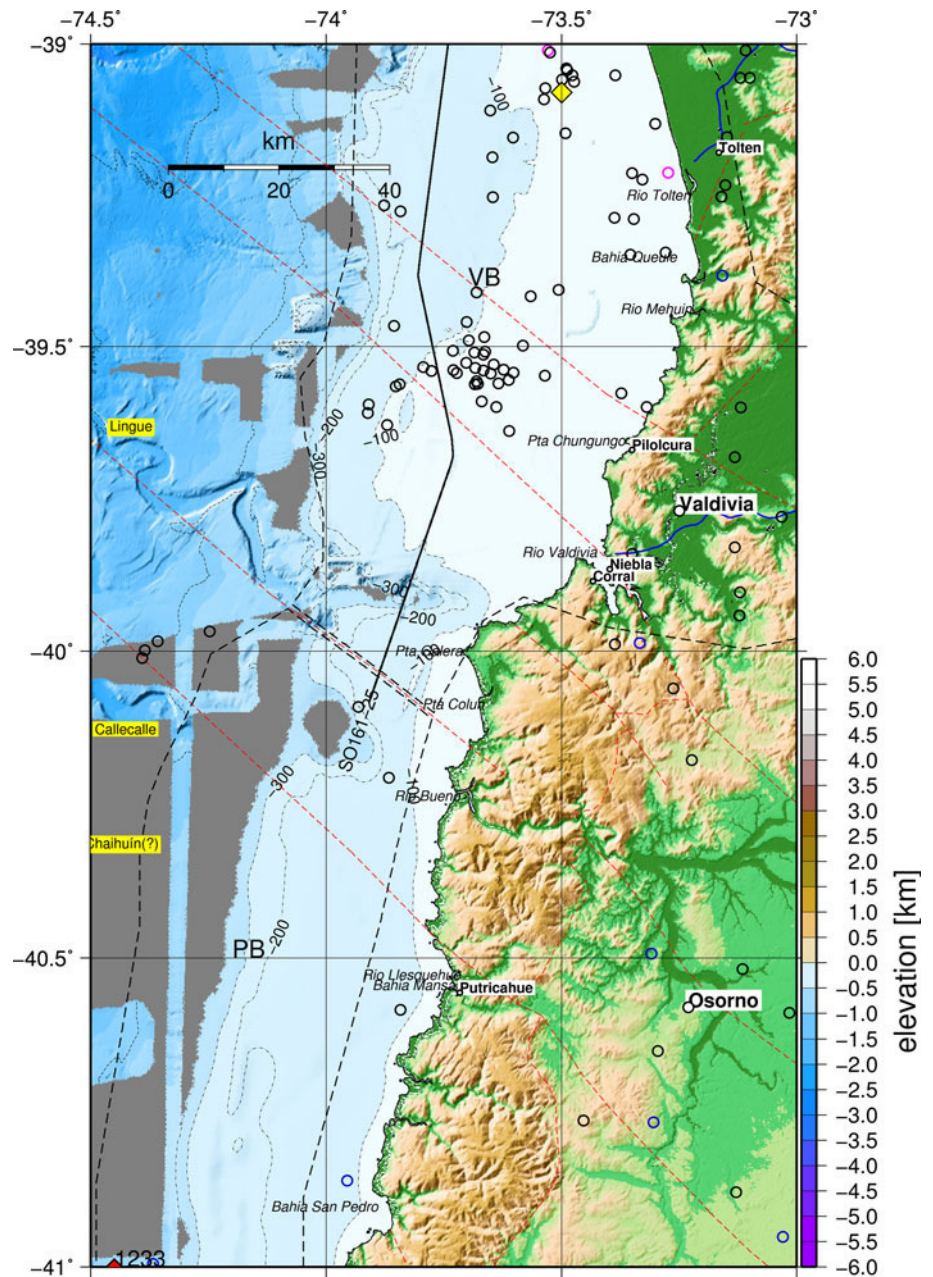


371 supposed to incise the shelf directly south of Mocha Island
 372 but is unresolved in our data set as we lack precise shelf
 373 bathymetry and as the slope is deformed by a giant slope
 374 failure (Geersen et al. 2011b); (9) Tolten Canyon might be
 375 related to the river systems of Tolten and Imperial, but we
 376 lack precise bathymetric data of the shelf area to test the
 377 relationship (Fig. 4); (10 and 11) Lingue Canyon and
 378 Calle Calle Canyon, two closely spaced submarine canyon
 379 systems lie offshore Valdivia: the northern one seems to be
 380 related to the exit of Río Valdivia, whereas the southern one
 381 might rather be connected to Río Bueno (Fig. 5). Both
 382 canyons were confusingly referred to as Río Bueno, Cal-
 383 le Calle or Tolten Canyons (Thornburg et al. 1990; Völker
 384 et al. 2006; Raitzsch et al. 2007; Rehak et al. 2008); (12)

385 Chaihuin Canyon south of Valdivia is not resolved in our
 386 data; (13) Chacao Canyon in continuation of the Chacao
 387 Channel (Fig. 6) and (14) Cucao Canyon offshore Chiloé
 388 Island (Fig. 6). As a number of the canyons cut deeply into
 389 the shelf, they should form effective traps for sediment that
 390 is transported coast-parallel on the shelf by bottom currents.

391 The role that canyon systems play in supplying sediment
 392 to the trench is evidenced by the submarine fan systems
 393 that exist at the exits of the larger canyons (Valdivia
 394 Canyon, Tolten Canyon, BioBio Canyon). These sub-
 395 marine fans are asymmetrical and their northern (down-
 396 slope) morphology contrasts to their southern (upslope)
 397 morphology as they have compositional structures (fan
 398 lobes) to the south and lag deposits and erosional structures

Fig. 5 Bathymetric map of the Chilean shelf and upper slope from 39°S to 41°S (Valdivia). *Black lines* indicate the position of seismic profiles of the SPOC project shot on RV SONNE cruise SO161 (Reichert 2002). *Circles* denote epicentres (*blue*: main and aftershocks of the Maule earthquake, Servicio Sismológico de Chile, ssn.dgf.uchile.cl/, *magenta*: Bohm et al. 2002, *black*: Dzierma et al. submitted) *Red stippled lines* show tectonic faults mapped on land between 36°S and 42°S by Melnick and Echtler (2006b). A *yellow diamond* refers to an exploration well, referenced in the text. *Stippled black lines* correspond to outlines of shelf basins. Absence of bathymetric information is indicated as *grey areas*



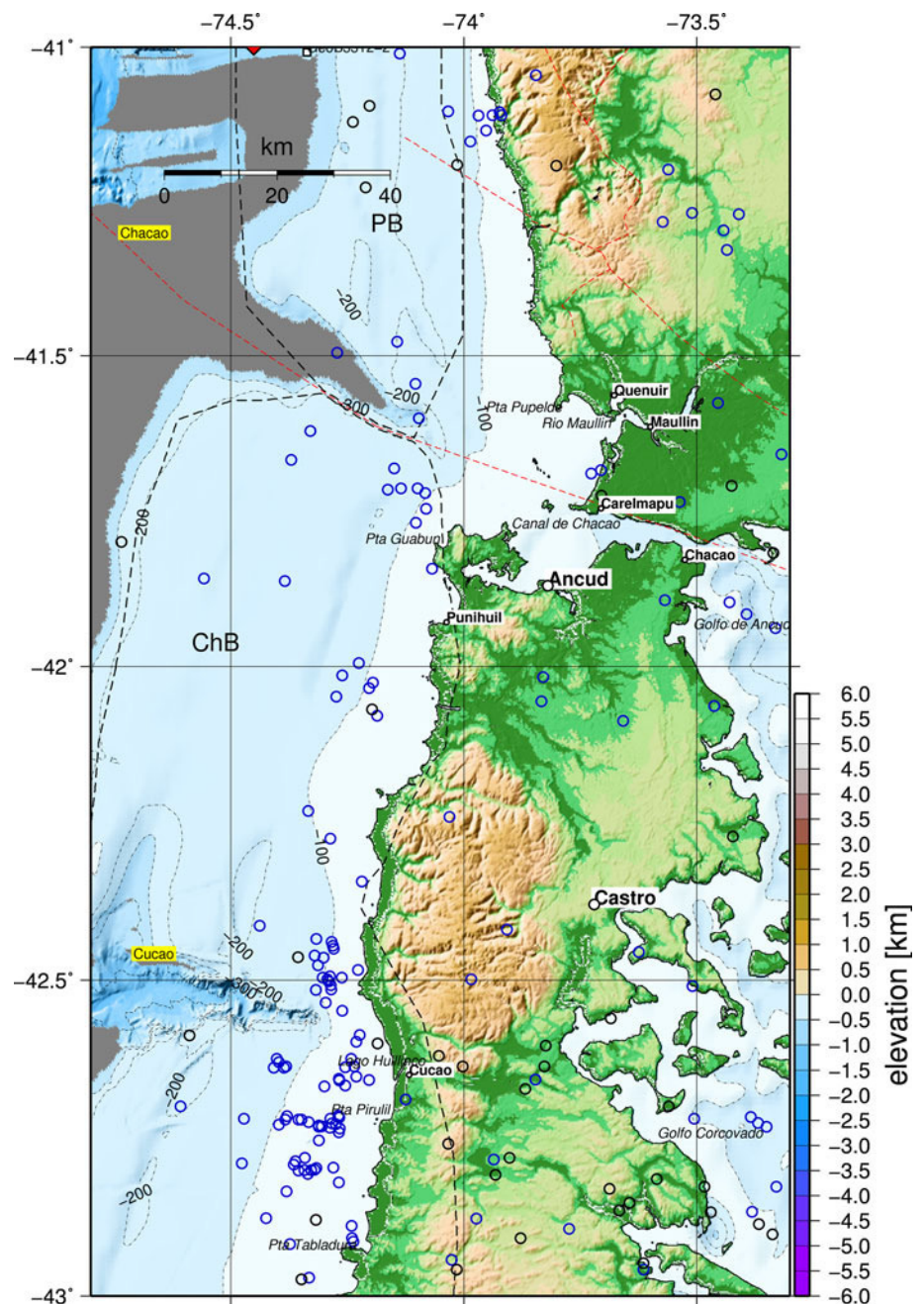
399 (furrows) to the north (Thornburg et al. 1990; Völker et al.
400 2006, 2008). Within the Peru–Chile Trench, a submarine
401 channel of 3–5 km width and up to 200 m depth (the Chile
402 Axial Channel) that is inclined northwards cuts into the
403 flat-lying trench sediments (Völker et al. 2006). At its
404 southern end, the channel appears to be in direct contin-
405 uation of the Chacao Canyon from where it continues
406 northward over more than 1,000 km to the Juan Fernández
407 Ridge and possibly beyond. The distributary channels of
408 most submarine fans connect directly to this axial channel,
409 in a way that it appears to form a natural northward path-
410 way for sediments that exit from the submarine canyons. At
411 the exit of the San Antonio Canyon, sediments have

412 ponded behind an accretionary ridge and were deposited as
413 overbank deposits to the south of a distributary channel that
414 breaches the ridge (Laurson and Normark 2002).

Forearc Basins and upper plate fault zones

415
416 Between 33°S and 43°S, a number of marine shelf forearc
417 basins are known from seismic and petroleum exploratory
418 well investigations of the Chilean state oil company
419 Empresa Nacional del Petróleo (ENAP) (Mordojovic 1981;
420 González 1989, Fig. 1). Two of these basins (Arauco and
421 Valdivia Basin) were covered by seismic sections of RV

Fig. 6 Bathymetric map of the Chilean shelf and upper slope from 41°S to 43°S (Chiloé Island). Circles denote epicentres (black: Dzierma et al. submitted, dark blue: Lange et al. 2007). Red stippled lines show tectonic faults mapped on land between 36°S and 42°S by Melnick and Echtler (2006b). Stippled black lines correspond to outlines of shelf basins. Absence of bathymetric information is indicated as grey areas



422 SONNE cruise SO161 (Reichert 2002) as part of the project
423 “Subduction Processes off Chile” (SPOC) in 2001. We
424 show a 375-km-long deep reflection seismic line (SO161-
425 25, Fig. 7) that roughly follows the trend of the coast
426 line (Figs. 3, 4, 5) in combination with the stratigraphic
427 information from Mordojovic (1981) and González (1989)
428 to document the structure of the two forearc basins.
429 We further trace the positions of upper plate faults in
430 the marine forearc and investigate their impact on basin
431 structure.

432 From North to South, shelf forearc basins are Navidad,
433 Chanco, Itata, Arauco, Valdivia, Pucatrihue and Chiloé

basins (Fig. 1). The basins have their respective depocentres
435 at the continental shelf, taper towards coast and trench
436 and are separated by basement highs. The creation of the
437 basins between 34 and 45°S is related to subsidence of the
438 present shelf and sectors of the slope by >1.5 km between
439 10.9 and 3.6 Ma (Melnick et al. 2009).

440 South of 38°S, the boundaries between the individual
441 forearc basins correlate with inferred marine continuation of
442 prominent upper plate faults (Figs. 4, 5, 6) that have been
443 described by Melnick and Echtler (2006b) and Melnick et al.
444 (2009). Upper plate faults that strike in SE–NW direction,
445 oblique to the convergence direction of the Nazca Plate, are

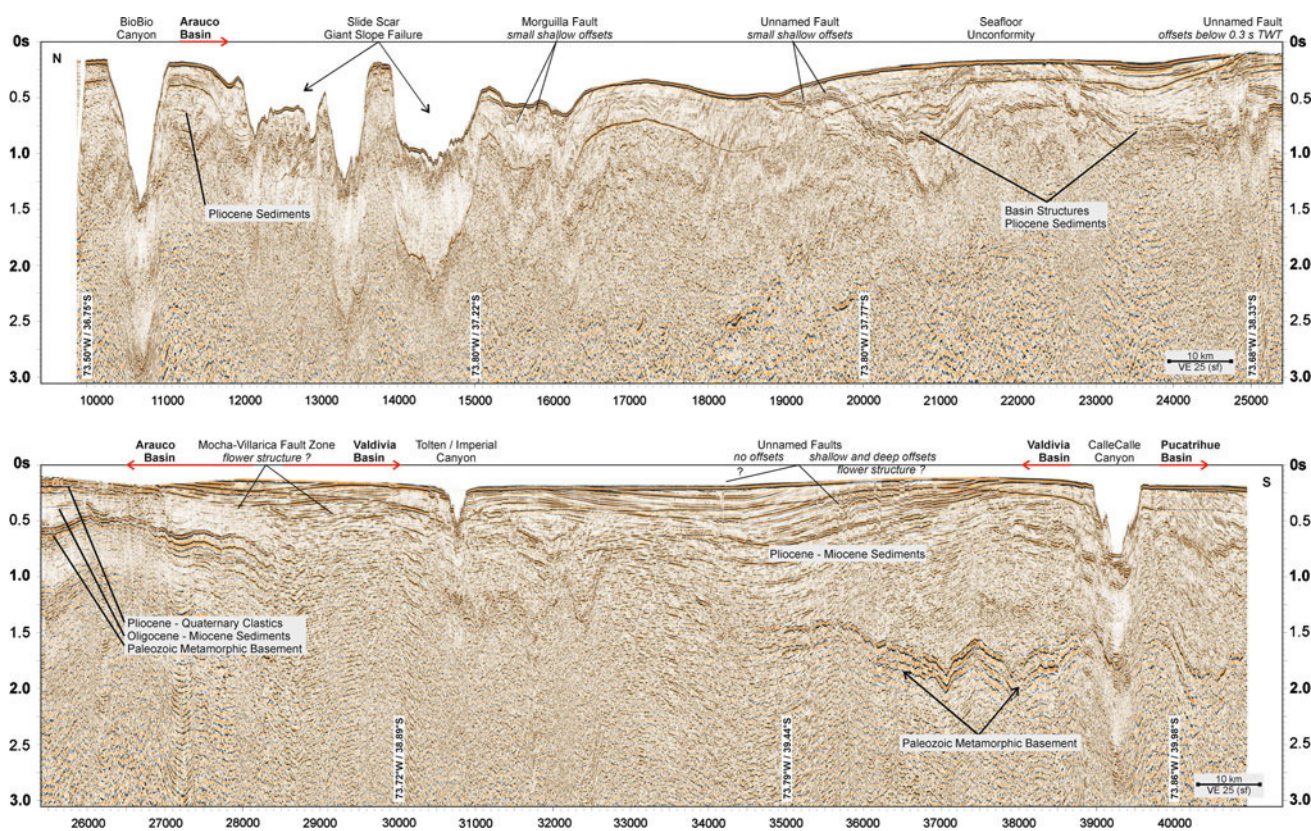


Fig. 7 Seismic reflection profile SO161-25 across Arauco and Valdivia Basins (Figs. 3, 4, 5) from 36.75°S to 38.33°S (*upper panel*) and 38.33°S to 40°S (*lower panel*) showing major tectonic structure and sedimentary units of the basins

446 likely the result of the northward motion of the Chiloe
447 Microplate and its collision with the South American Plate in
448 the region of the Arauco Peninsula (37.5°S). Some further
449 upper plate faults are located within individual basins.

450 The seismic section SO161-25 (Fig. 7) was acquired
451 with a recording time of 14 s two-way travel time (TWT).
452 It runs along the shelf in North–South direction from
453 36.75°S to 40°S along the axes of the Arauco Basin, the
454 Valdivia Basin and the northernmost area of the Pucatrihue
455 Basin (Figs. 3, 4, 5). As only a very small part of the entire
456 Pucatrihue Basin is imaged by the seismic line, the basin is
457 not discussed in detail.

458 Arauco Basin

459 The Arauco Basin extends over an area of 8,000 km² from
460 the latitude of Concepción in the North to the Mocha Island
461 in the South (Fig. 1). In seismic line SO161-25 (Fig. 7), it
462 is displayed from the start of the section to the common
463 midpoint (CMP) 28500 at $-73.693/-38.718$. Around CMP
464 10600 ($-73.559/-36.799$), the V-shaped BioBio Canyon
465 cuts about 900 m into the shelf. Between CMPs 11900 and
466 15100 ($-73.685/-36.905$ to $-73.804/-37.234$), the sea-
467 floor shows two depressions of 7 and 15 km width and up to
468 650 m depth, separated by a bathymetric high (at around

CMP 13700, $-73.790/-37.077$). The depressions represent
469 indentations that belong to the upslope part of a giant sub-
470 marine slope failure that removed more than 350 km³ of
471 slope sediment, continental framework rock and compacted
472 accretionary wedge material. The slope failure affected the
473 full width of the continental slope and shifted the shelf
474 break further landwards (Geersen et al. 2011b).
475

476 The Arauco Basin can be subdivided into a northern,
477 central and southern part based on the seismic reflection
478 pattern. In the northern part (start of the seismic section to
479 CMP 18500 at $-73.833/-37.608$), only the upper 0.5 s
480 TWT of the subsurface shows distinct seismic reflectors
481 that likely represent Pliocene sediments (all information
482 about stratigraphic units after Mordojovic 1974 and
483 González 1989). Towards greater depth, reflections appear
484 chaotic and disturbed. In this part of the seismic section,
485 it is impossible to locate the Palaeozoic metamorphic
486 basement. In the central part of the Arauco Basin (CMP
487 18500–25000, $-73.833/-37.608$ to $-73.678/-38.328$),
488 distinct reflectors are visible down to a depth of about 1 s
489 TWT. Seismic reflectors that again likely represent Plio-
490 cene sediments are heavily folded and form two basin
491 structures. At the flanks of the basins, reflections are
492 truncated by the seafloor unconformably. The southern part
493 of the Arauco Basin between CMPs 25000 and 28500

494 (−73.678/−38.328 to −73.693/−38.718) shows a distinctly different seismic reflection pattern. Here, some high-amplitude reflectors that likely represent Palaeozoic metamorphic basement are observed between depth of 495 0.5–0.75 s TWT. A zone of lower reflectivity on top of that unit may correspond to Oligocene–Miocene sediments, 496 whereas the shallowest subsurface is formed of Pliocene to 497 Quaternary clastic sediments. The latter unit is represented 498 by high-amplitude reflectors. In this area, the continental 499 shelf is exceptionally wide (up to 60 km) with Mocha 500 Island exposed up to 390 m above sea level. The proximity 501 of the Palaeozoic metamorphic basement to the seafloor 502 may be caused by high uplift rates in this area.

507 In the onshore area of the Arauco Basin, a series of 508 prominent SE–NW striking upper plate faults are described 509 that appear to continue into the marine forearc (all information 510 about position of continental faults from Melnick 511 and Echtler 2006b and Melnick et al. 2009) (Figs. 4, 5, 6). 512 Among those faults, the Morgüilla Fault is inferred to 513 intersect the seismic line SO161-25 around CMP 16000 514 (−73.827/−37.331). In this area, seismic reflectors in the 515 shallow subsurface are discontinuous, whereas towards 516 greater depth, no reflectors or seismic units are observed 517 that could indicate the position and the dip of the Morgüilla 518 Fault. Offsets in the seismic reflections in the shallow 519 subsurface indicate that the Morgüilla fault has been active 520 in the Pleistocene and Pliocene. Also, the Morgüilla fault 521 seems to develop into a flower structure in shallow depth as 522 is indicated by the presence of repeated small offsets.

523 Further to the south, two unnamed faults that branch into 524 a single fault zone in the continental forearc are inferred to 525 border the central part of the Arauco Basin. This area is 526 characterized by the folded basin structure between CMPs 527 18500 and 25000 (−73.833/−37.608 to −73.678/−38.328). 528 At the northern end of the basin structure, several small 529 (0.1–0.3 s TWT) offsets are observed down to a depth of 530 about 1 s TWT indicating ongoing deformation and faulting 531 since the Pleistocene. At the inferred position of the 532 southern branch of the unnamed fault between CMPs 24500 533 and 25000 (around −73.684/−38.300), the seismic signature 534 changes significantly. Here, the basin structure is 535 replaced by the high-amplitude reflections (at a depth of 536 0.5–0.75 s TWT) that likely represent the Palaeozoic 537 metamorphic basement in the southern part of the Arauco 538 Basin. Seismic reflections are truncated at various positions 539 in the subsurface. However, the shallowest reflectors (in the 540 upper 0.2 s TWT of the sub-seafloor) show no prominent 541 offsets, indicating that this fault has been inactive over the 542 Pleistocene.

543 The southern end of the Arauco Basin is located around 544 38.5°S at the Mocha-Villarica Fault Zone (MVFZ). 545 Here, the Palaeozoic metamorphic basement appears to be

suddenly truncated. Moreover, several small offsets are 546 observed in the shallow sedimentary sequence indicating 547 that the MVFZ possibly develops into a flower structure at 548 shallow depth and that activity has not ceased. 549

Valdivia Basin 550

The Valdivia Basin lies between Mocha Island in the North 551 and CalleCalle Canyon in the South and, like the Arauco 552 Basin, extends over an area of about 8,000 km². In seismic 553 section SO161-25 (Fig. 7), it is present from around CMP 554 28500 to CMP 39000 (−73.693/−38.718 to −73.816/ 555 −39.877). At around CMP 30750 (−73.736/−38.969), the 556 Tolten/Imperial Canyon cuts about 250 m into the shelf 557 sediments. Towards the south, the basin is bordered by the 558 CalleCalle Canyon that offsets the seafloor more than 559 500 m. In the southern part of the basin, high-amplitude 560 reflections between 1.5 and 2.0 s TWT depths likely indicate 561 the top of the Palaeozoic metamorphic basement. The 562 seismic signature of the continental basement is similar to 563 the one described for the southernmost part of the Arauco 564 Basin. Between CMP 28500 (−73.693/−38.718) and 565 35000 (−73.789/−39.443), the reflections of the Palaeo- 566 zoic metamorphic basement are lacking. Reflectors in the 567 upper part of the basin do not show offsets at CMP 35000, 568 which would indicate the presence of a fault zone, but 569 rather seem to fade away. Therefore, we speculate that the 570 cause of the absence of basement between CMP 35000 571 (−73.789/−39.443) and the southern end of the Arauco 572 Basin is that here the profile is located further offshore and 573 thus runs west of the seaward edge of the continental 574 basement. Layered seismic reflections that indicate the 575 presence of a thick sedimentary sequence, likely Pliocene 576 and Miocene sediments, are observed in the upper 577 0.5–1.5 s TWT of the subsurface over the entire Valdivia 578 Basin. This is in contrast to the Arauco Basin where the 579 sedimentary sequence is much thinner and the basement is 580 met at much shallower depth. 581

582 In the Valdivia Basin, two prominent, but unnamed 583 faults are known (Fig. 5) that could intersect the seismic 584 line SO161-25. At the position of the northern of these 585 unnamed faults around CMP 34000 (−73.797/−39.332), 586 no prominent offsets are observed in the seismic line, 587 indicating that faulting is not active here. At the position of 588 the southern fault around CMP 36000 (−73.760/−39.553), 589 the shallow sediments as well as the continental basement 590 are persistently offset up to 0.1 s TWT, indicating that this 591 fault develops in a series of parallel faults or a flower 592 structure at shallow depth. Faulting at this location seems 593 to be active, as offsets are found directly below the seafloor 594 reflection. Due to the lack of resolution in greater depth, it 595 is unclear how this fault evolves towards depth.

596 **Seismo-tectonics of the marine forearc**

597 The continental shelf of Southern Central Chile is tectonically deformed at different scales by different mechanisms
598 the common origin of which is the (oblique) plate convergence and subduction of the down-going plate. Here, we
599 combine information on epicentres from a number of local seismicological networks to provide a more uniform picture.
600 Data are from Dzierma et al. (submitted), Lange et al. (2007), Haberland et al. (2006) and Bohm et al. (2002). We
601 added epicentres of the main shock and aftershocks of the 1960 earthquake (Engdahl and Villaseñor 2002) as well as
602 of the 27 February of 2010, Mw 8.8 Maule earthquake (Servicio Sismológico de Chile, ssn.dgf.uchile.cl/). The
603 corresponding intra-crustal seismicity is partly diffuse, partly localized in clusters (Figs. 2, 3, 4, 5, 6). Basically,
604 three types of seismicity distributions can be observed in the marine forearc:

- 613 1. The trench-normal component of plate convergence leads to compressional deformation of shelf sediments
614 and continental basement. The megathrust, as a whole, is clearly visible in the seismicity distribution. Inside
615 the overriding forearc, however, the compression leads to a rather diffuse band of seismicity in which
616 individual faults are difficult to identify. The frequency of these forearc events is much higher north than south
617 of 36°S. Focal planes indicate mainly thrusting in the forearc on planes subparallel to the trench (e.g.
618 Barrientos 2007).
- 619 2. The northward motion of the Chiloé Microplate (or Chiloé Sliver, Melnick et al. 2009) with respect to the
620 stable Andean foreland to the east along the arc-parallel LOFZ decreases northwards from 46°S to
621 38°S (Rosenau et al. 2006; Wang et al. 2007). This velocity gradient may have been partly accommodated
622 by internal deformation of the Chiloé fore-arc sliver, consistent with contractional and transpressional fault
623 zones in the Arauco Region that strike oblique to the margin, such as the Lanalhue Fault and MVFZ
624 (Melnick and Echtler 2006a, b; Rosenau et al. 2006; Melnick et al. 2009). At some of these faults zones
625 clusters of seismicity are observed that locate down to lower crust and uppermost mantle levels (Dzierma
626 et al. submitted). Some clusters located offshore indicate that the marine forearc is getting sheared in
627 NW–SE direction in addition to the overall background compression. They show the offshore extrapolations
628 of the MVFZ south of Mocha Island (Haberland et al. 2006; Dzierma et al. submitted) and of a nameless fault
629 NW of Valdivia close to the slip maximum of the 1960 Valdivia earthquake (Dzierma et al. submitted). The
630 seismicity cluster along the

647 offshore extrapolation of the MVFZ may have been persistent between 2004 and 2009 because it was
648 observed by both Haberland et al. (2006) and Dzierma et al. (submitted).

- 649 3. Faulting of the down-going plate seems to continue from the outer rise—where it is related to plate
650 bending—until beneath the forearc where it is related to the megathrust process. This is evident from fault
651 displacements cutting through the entire overriding plate down into the plate interface as imaged by
652 seismic reflections (Sick et al. 2006). Linear seismicity clusters locating beneath the forearc near the plate
653 interface and in the down-going plate indicate that this faulting is an ongoing process (Dzierma et al. submitted).
654 Two of these clusters were found beneath the Valdivia Basin NW of Tolten and W of Mocha Island.

663 **Paleo-accretionary complex beneath the continental shelf**

664 Information on the structure of the continental crust that lies beneath the continental shelf and upper slope, under-
665 neath and seaward of the sedimentary basins has been obtained by seismic investigations over the last ~20 years
666 (e.g. Bangs and Cande 1997; Contreras-Reyes et al. 2008, 2010; Scherwath et al. 2009; Moscoso et al. 2011). Here,
667 we summarize recent observations on this issue.

668 Figure 8 shows a typical cross-section of the marine forearc off southern Central Chile. The frontal accretionary
669 prism is 5–40 km wide (Contreras-Reyes et al. 2010) and abuts the truncated continental basement (inner prism) that
670 extends seaward from beneath the shelf (Bangs and Cande 1997). This inner prism, presumably of Jurassic age, represents
671 a paleo-accretionary prism. This paleo-accretionary wedge in turn abuts the Paleozoic continental metamorphic
672 basement that is exposed on land in the Coastal Cordillera. The Coastal Cordillera south of 34°S is mainly built by two
673 units, the Western and Eastern Series, that constitute coeval parts of a Late Palaeozoic paired metamorphic belt
674 dominated by siliciclastic metasediments (Willner 2005). The Western Series represents a paleo-accretionary prism
675 and dominantly consists of HP/LT metasediments with subordinate metabasite intercalations” (see Willner 2005),
676 whereas the Eastern series is a belt of less deformed low-pressure/high-temperature metasediments that represent the
677 retro-wedge (Willner et al. 2005; Glodny et al. 2006).

678 The transition between the present accretionary prism and the sandwiched paleo-accretionary prism is visible in
679 seismic refraction data (Contreras-Reyes et al. 2008; Scherwath et al. 2009) and as a morphological transition
680 between rough lower slope and more smooth upper slope

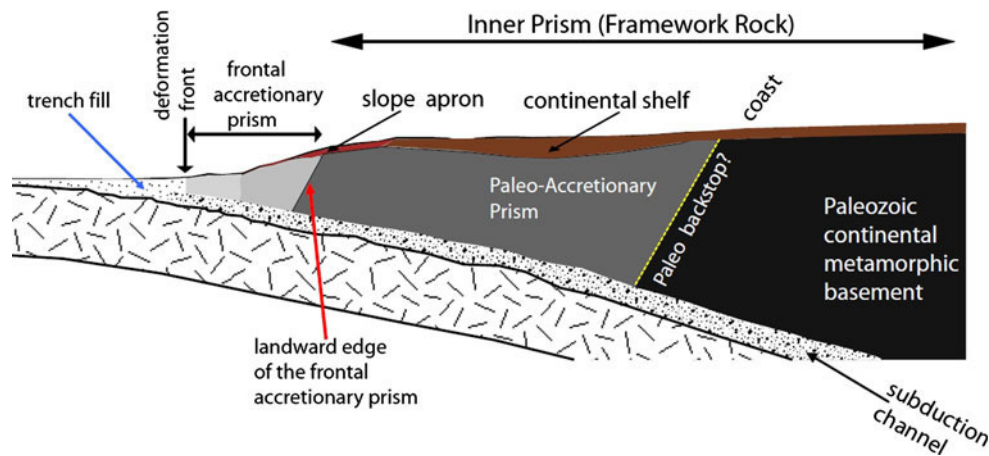


Fig. 8 Typical cross-section of the southern Central Chile convergent margin (after Contreras-Reyes et al. 2010). The frontal accretionary prism is typically 5–40 km wide and abuts against the present backstop, formed by the inner prism that is 50–80 km wide. The inner prism is likely composed of more than one rock unit. Seismic refraction (Contreras-Reyes et al. 2008; Scherwath et al.

2009) and seismological evidence (Haberland et al. 2006; Lange et al. 2007) show the presence of a paleo-backstop structure that separates a paleo-accretionary prism complex from the onshore exposed Paleozoic continental metamorphic basement (Hervé et al. 1988; Glodny et al. 2006)

696 morphology (Geersen et al. 2011a). The landward backstop
697 of the paleo-accretionary prism against continental meta-
698 morphic basement (paleo-backstop) is manifest as velocity
699 gradient suggesting a change in rock type (Contreras-Reyes
700 et al. 2008; Scherwath et al. 2009) as well as by intraplate
701 seismicity (Haberland et al. 2006, 2009; Lange et al. 2007;
702 Dzierma et al. submitted).

703 Exploratory wells of the Chilean state oil company
704 ENAP are located landward of the paleobackstop, so they
705 do not help in determining the composition and age of the
706 paleo-accretionary complex. The degree of consolidation
707 and lithification of the paleo-accretionary complex is
708 higher than that of the frontal accretionary prism but
709 lower than that of the Palaeozoic continental framework.
710 The remarkably high lateral velocity gradient from 5.5
711 to >6.0 km/s implies an abrupt change in rock type
712 (Contreras-Reyes et al. 2008), and hence alternation
713 between accretion and erosional phases. The size of the
714 paleo-accretionary complex could have been much larger
715 at the end of the accretion phase, when the complex was
716 formed. Thereafter, an integral part of the accretionary
717 complex was tectonically eroded (Kukowski and Oncken
718 2006). At present, the width of 50 km of the paleo-accre-
719 tionary complex represents the remaining material left after
720 the last erosional phase, which took place in the Miocene
721 according to Melnick and Echtler (2006a) and Encinas
722 et al. (2008). Assuming alternation between accretion and
723 erosion phases and based on the age of the oldest shelf
724 sediments (late Cretaceous), the estimated age for the
725 paleo-accretionary complex is Jurassic (Contreras-Reyes
726 et al. 2008).

Present shelf and slope sedimentation

The young sediment cover of the shelf and slope was
sampled over the last 20 years by coring campaigns along
depth transects (Table 1). ODP Leg 202 Sites 1233, 1234
and 1235 were drilled in slope basins of the upper and
middle slope in water depths of 838, 1,015 and 489 m,
respectively (Figs. 3, 5). Sediment-echosounder data were
obtained along cruise tracks of RV SONNE cruise SO161
and SO210 on the continental slope. These latter data are
presented here for the first time to image sedimentary
structures on the shelf.

The ODP coring had the goal to obtain an undisturbed
millennium-scale sediment core record of paleoclimatic
changes. Consequently, small slope basins with thick sed-
iment fill, where turbidites were expected to be channelled
away by surrounding canyons, were selected for drilling
(Mix et al. 2003). In this setting, thick and rapidly accu-
mulating hemipelagic sequences were cored, which are
characterized by extremely high bulk sedimentation rates of
90 cm/ka (site 1234), 70 cm/ka (site 1235) and >100 cm/ka
(site 1233) over the cored intervals. The lithology is
described as homogeneous silty clay and clay with varying,
but generally low biogenic content and few thin silt and
volcanic ash layers. The low biogenic component in spite of
persistent highly productive upwelling cells in the Con-
cepción area (sites 1234 and 1235) was explained by dilu-
tion due to the overwhelmingly high fluvial input of
siliciclastic material (Mix et al. 2003).

Surface sediment samples (grab samples, gravity cores
and multicorer samples) of shelf and upper slope were

757 described by Lamy et al. (1998, 1999, 2001), Hebbeln et al.
 758 (2000), Muñoz et al. (2004), Raitzsch et al. (2007) and
 759 Stuut et al. (2007). Sediment composition of the described
 760 samples is dominated by terrigenous input which generally
 761 increases to the south in relation to the climatically con-
 762 trolled southward increase in denudation rates of the hin-
 763 terland. Offshore mid-latitude Chile (33°S) samples
 764 provide a record of temporal variations in the terrigenous
 765 sediment supply that reflect changes in weathering condi-
 766 tions related to shifts of the latitudinal position of the
 767 Southern Westerlies (Lamy et al. 1999, 2001). Lamy et al.
 768 (1998) showed that regional variations in silt size and bulk
 769 mineralogy of terrigenous silts are governed by the source-
 770 rock composition of the different geological terranes and
 771 the relative source-rock contribution of the Coastal Cor-
 772 dillera and the Andes as controlled by the river networks.
 773 These trends are also reflected in the bulk chemistry (Stuut
 774 et al. 2007).

775 The biogenic sediment input shows a close relation to the
 776 environmental conditions in the Peru–Chile Current, as the
 777 accumulation rate of organic carbon in the sediments fits
 778 well with the present-day productivity patterns that are
 779 related to cells of coastal upwelling known from satellite
 780 data (Hebbeln et al. 2000). The carbonate content along the
 781 slope varies mainly between 0 and 20 % (Hebbeln et al.
 782 2000). For the continental slope offshore Concepción,
 783 sedimentation rates were determined over the past ~100
 784 years for two sites at 1,294 and 2,065 m water depth
 785 (Muñoz et al. 2004). The very high values of 180 ± 20
 786 cm/ka were explained by the vicinity of the BioBío Canyon.

787 Seismic reflection data (Contardo et al. 2008; Geersen
 788 et al. 2011b), bathymetric data (Völker et al. 2011a, b) and
 789 the PARASOUND sediment-echosounder data shown here
 790 demonstrate that mass-wasting is a common effect on the
 791 slope that affects many of the slope basins and that
 792 focusing of sedimentation leading to extreme sedimenta-
 793 tion rates in sheltered slope basins is contrasted by win-
 794 nowing and sediment starved zones on the shelf. PARASOUND
 795 sediment echo-sounder data of the shelf
 796 break and uppermost slope around 36°S show a thin sedi-
 797 ment cover that unconformably overlies deformed and til-
 798 ted older strata (Fig. 9a, b). Locally, the older strata pinch
 799 out to form hard ground basement highs lacking a young
 800 sedimentary cover. Further south around 38°S, the rela-
 801 tively thin young sediment cover is affected by bottom
 802 current erosion as can be seen from v-shaped incisions
 803 (Fig. 9c). Deformation of the topmost sediment cover
 804 due to mass wasting is common (Fig. 9d). The overall
 805 impression of the sediment-echosounder data is of a bot-
 806 tom-current-dominated high energetic depositional regime
 807 where young sediments fill sheltered basins and pockets
 808 while elevated areas are practically swept free from
 809 young sediments and/or subject to bottom current erosion.

Probably a large fraction of the shelf sedimentation is 810
 exported to shelf basins or eventually funnelled to the 811
 Peru–Chile Trench via submarine canyons. On the shelf, 812
 offshore Punta Ligure (~36°S, Fig. 3) on the other hand, 813
 undisturbed and well-stratified sediments of 50-ms two- 814
 way-travel time were observed on RV SONNE cruise 815
 SO210 (Linke 2011). 816

Gas and fluid seepage 817

The presence of solid gas hydrates is indicated by the 818
 observation of a bottom simulating reflector (BSR) in 819
 seismic reflection data, while the seepage of gas-charged 820
 fluids at the seafloor is manifest by the occurrence of 821
 chemosynthetic bio-communities as well as by the acoustic 822
 detection of gas bubbles in the water column (acoustic 823
 flares in sediment-echosounder data). Here, we report on 824
 the present-day knowledge on the distribution of seepage- 825
 related fauna. At other convergent continental margins, 826
 such as of Central America and New Zealand, active 827
 seepage of (methane-rich) fluids is a common phenome- 828
 non, often located within a trench-parallel belt of the 829
 middle continental slope. In those places, a variety of 830
 active seeps appear to be long-standing structures, related 831
 to faults that connect the plate interface with the seafloor 832
 and form conduits (e.g. Sahling et al. 2008; Barnes et al. 833
 2010). The presence of fluid seepage can therefore bear 834
 information on the hydraulic properties of the forearc, its 835
 tectonic situation and internal structure. 836

Seismic profiles show bottom simulating reflectors 837
 (BSR), commonly associated with the occurrence of gas 838
 hydrates on the continental slope of southern Central Chile 839
 below a water depth of 650 m (Brown et al. 1996; Díaz- 840
 Naveas 1999; Grevenmeyer et al. 2003; Morales 2003; 841
 Rodrigo et al. 2009). At some places, the BSR intercepts 842
 the seafloor below the shelf break (Rodrigo et al. 2009). 843
 Typical members of chemosynthetic bio-communities 844
 indicative for methane seepage (e.g. clams of the family 845
Vesicomidae and tubeworms of the genus *Lamellibrachia*) 846
 are known by now from many places at the Chile margin. 847
 The first indication of seep communities was the descrip- 848
 tion of *Calyptogena australis*, from the vicinities of Mocha 849
 Island (~38°S) at 1,400 m water depth (Stuardo and 850
 Valdovinos 1988, Fig. 4). This first report was followed 851
 by others from offshore Concepción Bay (Sellanes and 852
 Krylova 2005; Oliver and Sellanes 2005; Sellanes et al. 853
 2008; Quiroga and Sellanes 2009), a region that was 854
 termed the Concepción methane seep area (CMSA, 855
 Sellanes et al. 2004, Fig. 3). Three other bathyal seep sites 856
 were discovered recently, located off the Limari River (at 857
 ~30°S) at 1,000 m depth, off El Quisco (~33°S) at 350 m 858
 depth, and the most recent one, off the Taitao Peninsula 859

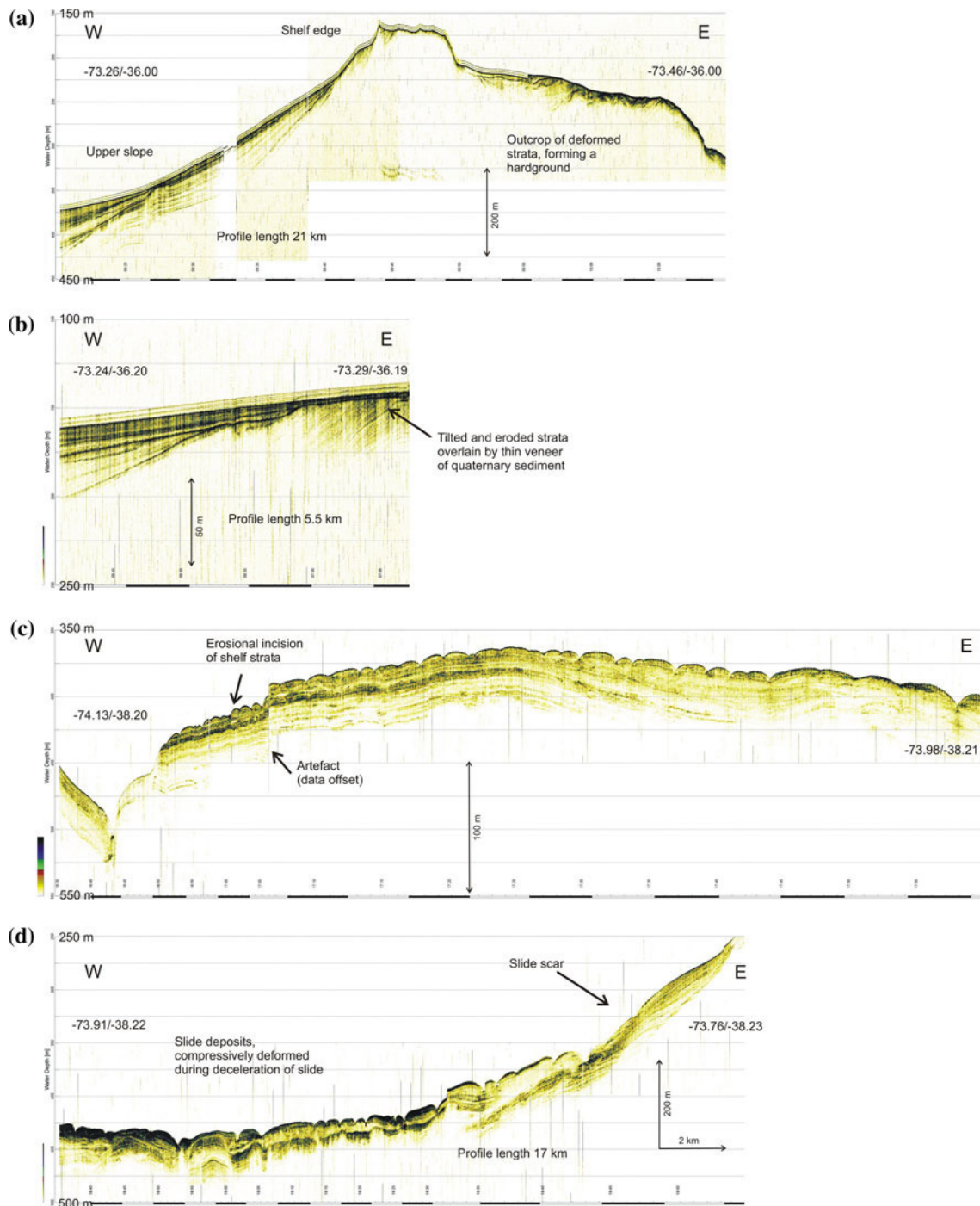


Fig. 9 Sample PARASOUND sediment-echosounder profiles from the shelf and upper slope of southern Central Chile, each representing seismic facies types. **a** Outcrop of lithified sediments at the shelf edge; **b** angular unconformity of tilted lithified strata against thin

cover of young sediments; **c** subparallel strata, incised by parallel grooves; **d** small landslide at the shelf edge. Location of PARASOUND profiles **a** and **b** is indicated in Fig. 3, of profiles **c** and **d** in Fig. 4

860 (~46°S) at 600 m depth (J. Sellanes, unpublished data), all
 861 of them indicated by the presence of typical seep communities.
 862 Fluid seepage-related features of the seafloor
 863 (patches of high acoustic backscatter, possibly representing
 864 authigenic carbonates) as well as acoustic anomalies in the

water column (gas flares) were detected on the upper to
 middle slope in 1,500 m water depth (Flueh and Bialas
 2008) offshore Concepción Bay (CMSA, Fig. 3). While
 authigenic carbonates that probably formed as the result of
 methane-rich fluid expulsion form extensive pavements in

865
 866
 867
 868
 869

two distinct areas of the middle slope (north of BioBio Canyon and around Itata Canyon), acoustic anomalies in the water were described rarely (Klaucke et al. 2012). According to Klaucke et al. (2012), the apparent misfit between indications of present fluid seepage and the size of authigenic carbonate patches and chemohierms indicates that fluid venting must have been more intense over some period of the past.

Chloride content of the pore waters of gravity cores from the continental slope is meaningful for the detection of subduction-related diagenetic processes, as a number of these processes consume (alteration of volcanic ash to smectite, Martin et al. 1995) or release (transformation of smectite to illite, Kastner et al. 1991) fresh water when trench fill is being subducted along with the down-going plate (e.g. Hensen et al. 2004). Offshore Central Chile, pore water geochemical measurements from gravity cores obtained on RV SONNE cruise SO210 (Linke 2011) were conducted by Scholz et al. (submitted). They show that pore fluids in cores of the accretionary prism show a higher chlorinity than seawater and relate this finding to the sequestration of water through formation of hydrous minerals (alteration of volcanic ash to smectite). In contrast, cores from the upper slope have a lower chlorinity than seawater which most likely is due to clay mineral dehydration, for example the alteration of smectite to illite. Thermal constraints from heat flow modelling let Scholz et al. (submitted) suggest that these low-salinity fluids are generated in the upper plate, whereas the dehydration of underthrust sediments must take place further seaward.

The occurrence of gas seeps is also known at many intertidal and shallow subtidal places at the W side of Mocha Island off southern Central Chile (~38°S, Fig. 4). At this locality, two possible sources have been ascribed for it: (a) subsurface thermogenic hydrocarbon accumulations that are trapped within the Cretaceous rock sequence (Comisión Nacional de Energía Chile, 2002; Sánchez 2004) and (b) coal-bed methane, coming from coal-bearing sediments of the Trihuco Formation in the Arauco Basin in the continental shelf (Mordojovic 1981). Recent measurements indicate that emanations contain 70 % methane, and the estimated methane fluxes emitted directly to the atmosphere amount to 815 ta^{-1} when considering the five subtidal and intertidal seeps detected at the Island (Jessen et al. 2011). The C stable isotope compositions of methane from the intertidal seeps averaged at $-43.8 \pm 0.4 \text{ ‰}$ (with respect to PeeDee Belemnite) and are suggestive of a substantial fraction derived from thermogenic sources. While stable carbon isotopic compositions of marine benthic organisms indicate a dominant photosynthesis-based food web, $\delta^{13}\text{C}$ of some hard-substrate invertebrates were in the range -36.8 to -48.8 ‰ , suggesting assimilation of methane-derived carbon by some selected taxa (Jessen et al. 2011).

Summary and conclusion

Our compilation of older and recently published data, cruise reports, scientific theses and previously unpublished geological and geophysical data on the shelf and upper slope of Central Chile allows drawing the following conclusions:

1. The presence of fourteen deeply incised submarine canyon systems, their extension onto the shelf, as well as their direct connection to river systems on land impacts severely on shelf sedimentation, as the bulk of fluvial transported sediment is likely funnelled down-slope instead of being stored on the shelf. High sedimentation rates are observed on shelf and upper slope in spite of this deprivation of fluvial transported material due to local zones of constant or seasonal upwelling and due to the sheer amount of fluvial input. Sediment-echosounder profiles show both patches of undisturbed and well-stratified sediments on the shelf and eroded sedimentary structures closer to the shelf edge. The local lack of young sedimentary cover is attributed to the Gunther Current that flows vigorously poleward close to the shelf edge.
2. The sedimentary basins that underlie the shelf platform and the upper continental slope consist of Oligocene to Quaternary infill in structural basins of the Paleozoic metamorphic basement. The thickness of the individual units varies significantly both within Arauco and Valdivia Basin as well as from basin to basin. Reflectors of the sedimentary fill of those basins are offset by six fault zones that form the continuations of large crustal fault systems known on land such as the Morgüilla Fault and the Mocha-Villarica Fault Zone. The continuity of these SE-NW trending crustal faults into the submarine forearc has been postulated but never clearly documented before. Five of the six fault systems appear to have been active over the evolution of the basin from late Cretaceous to the present, while for one fault system activity appears to have ceased in Pleistocene. Some of these faults zones—notably the MVFZ (Haberland et al. 2006, offshore Arauco peninsula; Dzierma et al. submitted, cluster G), a nameless fault NW of Valdivia (Dzierma et al. submitted, cluster F) and side branches near the LOFZ (Dzierma et al. submitted, cluster H)—show clusters of seismicity that extend downwards into the lower crust, Moho and uppermost mantle. The clusters indicate that the marine forearc is getting sheared in NW–SE direction in addition to the overall background compression, a tectonic regime that is due to the transpressional docking of the Chiloé Microplate to the South American Plate.

- 974 3. The structure of the upper continental margin beneath
975 the shelf basins is marked by a prominent transition
976 from a former accretionary prism that was tectonically
977 eroded in parts to the newly forming accretionary
978 prism. This transition marks the shift from a phase of
979 tectonic erosion to the present phase of accretion that
980 is supposed to have occurred about 4 Ma ago. The
981 transition is further expressed in the surface morphol-
982 ogy as a shift from smooth, gently sloping upper
983 continental slope to a more complex and steeper slope
984 below 2,000 m water depth.
- 985 4. Seepage of gas-charged fluids is observed both indi-
986 rectly and directly, clustered to a few locations on the
987 shelf and upper slope. This seepage appears to be of
988 shallow origin and not related to the release of fluids
989 from the subducting Nazca Plate by deeply connecting
990 conduits as was observed, for example off Costa Rica
991 (Sahling et al. 2008).

992 **Acknowledgments** Part of the research off Central Chile was fun-
993 ded by the Fondo Nacional de Desarrollo Científico y Tecnológico
994 (FONDECYT) grants 1100166 (CMSA) and grant 1080623 (Mocha
995 Island), to Javier Sellanes and Silvio Pantoja, respectively. The pro-
996 ject SPOC (Subduction Processes off Chile) including the RV
997 SONNE cruise SO161 was funded by the German Federal Ministry of
998 Education and Research (BMBF) grant no. 03G0161A. We gratefully
999 acknowledge the help of the Dpto. de Geofísica de la Subdirección
1000 Nacional de Geología de SERNAGEOMIN (Servicio Nacional de
1001 Geología y Minería de Chile) that provided us with a bathymetric grid
1002 of the shelf areas of Chile. Some figures were created with The
1003 Generic Mapping Tools (GMT). We are grateful for helpful com-
1004 ments and thorough reviews by Juan Díaz-Naveas and an anonymous
1005 second reviewer. This publication is contribution no. 226 of the
1006 Sonderforschungsbereich 574 “Volatiles and Fluids in Subduction
1007 Zones” at Kiel University.

1008 References

- 1009 Angermann D, Klotz J, Reigber C (1999) Space-geodetic estimation
1010 of the Nazca-South America Euler vector. *Earth Planet Sci Lett*
1011 171:329–334
- 1012 Atkinson LP, Valle-Levinson A, Figueroa D, Pol-Holz RD, Gallardo
1013 VA, Schneider W, Blanco JL, Schmidt M (2002) Oceanographic
1014 observations in Chilean coastal waters between Valdivia and
1015 Concepción. *J Geophys Res* 107. doi:10.1029/2001JC000991
- 1016 Bangs NL, Cande SC (1997) Episodic development of a convergent
1017 margin inferred from structures and processes along the southern
1018 Chilean margin. *Tectonics* 16:489–503
- 1019 Barnes PM, Lamarche G, Bialas J, Henrys S, Pecher I, Netzeband GL,
1020 Greiner J, Mountjoy JJ, Pedley K, Crutchley G (2010) Tectonic
1021 and geological framework for gas hydrates and cold seeps on the
1022 Hikurangi subduction margin, New Zealand. *Marine Geol*
1023 272:26–48
- 1024 Barrientos SE (2007) Earthquakes in Chile. In: Moreno T, Gibbons W
1025 (eds) *The geology of Chile*. The Geological Society, London,
1026 pp 263–287
- 1027 Barrientos SE, Ward SN (1990) The 1960 Chile earthquake: inversion
1028 for slip distribution from surface deformation. *Geophys J Int*
1029 103:589–598

- Berger WH, Fischer K, Lai G, Wu G (1987) Ocean productivity and
1030 organic carbon flux. Part I. Overview and maps of primary
1031 production and export production. *Scripps Inst Oceanogr Ref*:
1032 87–30
- Bilek SL (2010) Seismicity along the South American subduction
1033 zone: review of large earthquakes, tsunamis, and subduction
1034 zone complexity. *Tectonophysics* 495:2–14
- Blumberg S, Lamy F, Arz HW, Echter HP, Wiedicke M, Haug GH,
1035 Oncken O (2008) Turbiditic trench deposits at the South-Chilean
1036 active margin: a Pleistocene–Holocene record of climate and
1037 tectonics. *Earth Planet Sci Lett* 268:526–539
- Bohm M, Luth S, Echter H, Asch G, Bataille K, Bruhn C, Rietbrock
1038 A, Wigger P (2002) The Southern Andes between 36 degrees
1039 and 40 degrees S latitude: seismicity and average seismic
1040 velocities. *Tectonophysics* 356:275–289
- Brown KM, Bangs NL, Froelich PN, Kvenvolden KA (1996) The
1041 nature, distribution, and origin of gas hydrate in the Chile Triple
1042 Junction region. *Earth Planet Sci Lett* 139:471–483
- Cáceres M, Valle-Levinson A, Atkinson L (2003) Observations of
1043 cross-channel structure of flow in an energetic tidal channel.
1044 *J Geophys Res* 108:3114
- Caress DW, Spitzak SE, Chayes DN (1996) Software for multibeam
1045 sonars. *Sea Technol* 37:54–57
- Cembrano J, Schermer E, Lavenu A, Sanhueza A (2000) Contrasting
1046 nature of deformation along an intra-arc shear zone, the Liquiñe–
1047 Ofqui fault zone, southern Chilean Andes. *Tectonophysics*
1048 319:129–149
- Cifuentes IL (1989) The 1960 Chilean earthquakes. *J Geophys Res*
1049 94:665–680
- Cisternas M, Atwater BF, Torrejon F, Sawai Y, Machuca G, Lagos M,
1050 Eipert A, Youlton C, Salgado I, Kamataki T, Shishikura M,
1051 Rajendran CP, Malik JK, Rizal Y, Husni M (2005) Predecessors
1052 of the giant 1960 Chile earthquake. *Nature* 437:404–407
- Contardo X, Cembrano J, Jensen A, Díaz-Naveas J (2008) Tectono-
1053 sedimentary evolution of marine slope basins in the Chilean
1054 forearc (33°30′–36°50′S): insights into their link with the
1055 subduction process. *Tectonophysics* 459:206–218
- Contreras-Reyes E, Grevemeyer I, Flueh ER, Reichert C (2008)
1056 Upper lithospheric structure of the subduction zone offshore of
1057 southern Arauco peninsula, Chile, at ~38°S. *J Geophys Res*
1058 113. doi:10.1029/2007JB005569
- Contreras-Reyes E, Flueh E, Grevemeyer I (2010) Tectonic control on
1059 sediment accretion and subduction off south-central Chile.
1060 *Tectonics* 29. doi:10.1029/2010TC002734
- Daneri G, Dellarossa V, Quiñones R, Jacob B, Montero P, Ulloa O
1061 (2000) Primary production and community respiration in the
1062 Humboldt current system off Chile and associated oceanic areas.
1063 *Marine Ecol Progr Series* 197:41–49
- Díaz-Naveas JL (1999) Sediment subduction and accretion at the
1064 Chilean Convergent Margin between 35°S and 40°S. PhD thesis,
1065 Christian-Albrechts University, Kiel
- Djurfeldt L (1989) Circulation and mixing in a coastal upwelling
1066 embayment; Gulf of Arauco, Chile. *Cont Shelf Res* 9:1003–1016
- Dzierma Y, Thorwart M, Rabbel W, Siegmund C, Comte D, Bataille
1067 K, Iglesia P, and Prezzi C (submitted) Seismicity near the slip
1068 maximum of the 1960 Mw 9.5 Valdivia earthquake (Chile): plate
1069 interface lock and active faults within the crust and subducted
1070 slab. *J Geophys Res* (Submitted to)
- Encinas A, Finger KL, Nielsen SN, Lavenu A, Buatois LA, Peterson
1071 DE, Le Roux JP (2008) Rapid and major coastal subsidence
1072 during the late Miocene in south-central Chile. *J S Am Earth Sci*
1073 25:157–175
- Engdahl ER, Villaseñor A (2002) Global seismicity: 1900–1999. In:
1074 Lee WHK, Kanamori H, Jennings PC, Kisslinger C (eds)
1075 *International handbook of earthquake and engineering seismol-
1076 ogy, part A, Chap. 41*. Academic Press, London, pp 665–690

- 1096 Fariás M, Charrier R, Carretier S, Martinod J, Fock A, Campbell D, Cáceres J, Comte D (2008) Late Miocene high and rapid surface uplift and its erosional response in the Andes of central Chile (33°S–35°S). *Tectonics* 27:TC1005
- 1097 Fariás M, Comte D, Roecker S, Carrizo D, Pardo M (2011) Crustal extensional faulting triggered by the 2010 Chilean earthquake: the Pichilemu Seismic Sequence. *Tectonics* 30:TC6010
- 1098 Farr TG, Rosen PA, Caro E, Crippen R, Duren R, Hensley S, Kobrick M, Paller M, Rodriguez E, Roth L, Seal D, Shaffer S, Shimada J, Umland J, Werner M, Oskin M, Burbank D, Alsdorf D (2007) The shuttle radar topography mission. *Rev Geophys* 45:1–33
- 1099 Fekete BM, Vörösmarty CJ, Grabs W (2000) Global composite runoff fields based on observed river discharge and simulated water balances. Complex Systems Research Center, University of New Hampshire. UNH-GRDC Composite Runoff Fields v1.0
- 1100 Figueroa D, Moffat C (2000) On the influence of topography in the induction of coastal upwelling along the Chilean Coast. *Geophys Res Lett* 27:3905–3908
- 1101 Flueh ER (1995) Fahrtbericht SO 103/cruise report SO 103, CONDOR 1 B. GEOMAR-Report 41:1–140 (Kiel)
- 1102 Flueh E, Bialas J (2008) RRS JAMES COOK Cruise Report JC23-A & B, IFM-GEOMAR, Kiel. doi:10.3289/ifm-geomar_rep_20_2008
- 1103 Flueh E, Grevemeyer I (2005) FS SONNE Cruise Report SO 181 Tipteq - from the incoming plate to megathrust earthquakes. Berichte aus dem Leibniz-Institut für Meereswissenschaften an der Christian-Albrechts-Universität zu Kiel 42:1–539. doi:10.3289/IFM-GEOMAR_REP_42_2011
- 1104 Flueh ER, Vidal N, Ranero CR, Hojka A, von Huene R, Bialas J, Hinz K, Cordoba D, Danobeitia JJ, Zelt C (1998) Seismic investigation of the continental margin off- and onshore Valparaiso, Chile. *Tectonophysics* 288:251–263
- 1105 Flueh E, Kopp C, Schreckenberger B (2002) RV SONNE Cruise Report SO161-1&4. GEOMAR Report 44:1–383
- 1106 Fossing H, Gallardo VA, Jørgensen BB, Hüttl M, Nielsen LP, Schulz H, Canfield DE, Forster S, Glud RN, Gundersen JK, Küver J, Ramsing NB, Teske A, Thamdrup B, Ulloa O (1995) Concentration and transport of nitrate by the mat-forming sulphur bacterium *Thioploca*. *Nature* 374:713–715
- 1107 Geersen J, Behrmann JH, Völker D, Krastel S, Ranero CR, Diaz-Naveas J, Weinrebe WR (2011a) Active tectonics of the South Chilean marine forearc (35°S–40°S). *Tectonics*:TC3006. doi:10.1029/2010TC002777
- 1108 Geersen J, Völker D, Behrmann JH, Reichert C, Krastel S (2011b) Pleistocene giant slope failures offshore Arauco Peninsula, Southern Chile. *J Geol Soc* 168(6):1237–1248. doi:10.1144/0016-76492011-027
- 1109 Glodny J, Echter H, Figueroa O, Franz G, Gräfe K, Kemnitz H, Kramer W, Krawczyk C, Lohrmann J, Lucassen F, Melnick D, Rosenau M, Seifert W (2006) Long-term geological evolution and mass-flow balance of the South-Central Andes. In: The Andes-Active subduction Orogeny. Springer, Berlin, pp 401–428
- 1110 González E (1989) Hydrocarbon resources in the coastal zone of Chile. In: Ericksen G (ed) *Geology of the Andes and its relation to hydrocarbon and mineral resources*. Circum-Pacific Council for Energy and Mineral Resources, Houston, TX, pp 383–404
- 1111 Grevemeyer I, Diaz-Naveas JL, Ranero CR, Villinger HW (2003) Heat flow over the descending Nazca plate in central Chile, 32 degrees S to 41 degrees S: observations from ODP Leg 202 and the occurrence of natural gas hydrates. *Earth Planet Sci Lett* 213:285–298
- 1112 Haberland C, Rietbrock A, Lange D, Bataille K, Hofmann S (2006) Interaction between forearc and oceanic plate at the South-Central Chilean margin as seen in local seismic data. *Geophys Res Lett* 33:L23302. doi:23310.21029/22006GL028189
- 1113 Haberle SG, Lumley SH (1998) Age and origin of tephras recorded in postglacial lake sediments to the west of the southern Andes, 44°S to 47°S. *J Volcanol Geothermal Res* 84:239–256
- 1114 Hagen RA, Vergara H, Naar DF (1996) Morphology of San Antonio submarine canyon on the Central Chile forearc. *Marine Geol* 129:197–205
- 1115 Haschke M, Sobel ER, Blisniuk P, Strecker MR, Warkus F (2006) Continental response to active ridge subduction. *Geophys Res Lett* 33:L15315
- 1116 Hebbeln D (2001) PUCK: report and preliminary results of R/V Sonne Cruise SO 156, Valparaiso (Chile)-Talcahuano (Chile), March 29-May 14, 2001. Berichte aus dem Fachbereich Geowissenschaften der Universität Bremen 182:1–195
- 1117 Hebbeln D, Wefer G (1995) Cruise Report of R/V SONNE Cruise 102, Valparaiso–Valparaiso, 9(May), pp 1995–28, June 1995. Berichte Fachbereich Geowissenschaften Universität Bremen 68:1–126
- 1118 Hebbeln D, Marchant M, Freudenthal T, Wefer G (2000) Surface sediment distribution along the Chilean continental slope related to upwelling and productivity. *Marine Geol* 164:119–137
- 1119 Heberer B, Roeser G, Behrmann JH, Rahn M, Kopf AJ (2010) Holocene sediments from the Southern Chile Trench; a record of active margin magmatism, tectonics and palaeoseismicity. *J Geol Soc Lond* 167:539–553. doi:10.1144/0016-76492009-015
- 1120 Hensen C, Wallmann K, Schmidt M, Ranero CR, Suess E (2004) Fluid expulsion related to mud extrusion off Costa Rica—a window to the subducting slab. *Geology* 32(3):201–204
- 1121 Hervé FE, Munizaga F, Parada MA, Brook M, Pankhurst R, Spelling N, Drake R (1988) Granitoids of the coast range of central Chile: geochronology and geologic setting. *S Am Earth Sci J* 1:185–194
- 1122 Hildreth W, Drake RE (1992) Volcán Quizapu, Chilean Andes. *Bull Volcanol* 54:93–125
- 1123 Hildreth W, Grunder AL, Drake RE (1984) The Loma Seca Tuff and the Calabozos caldera: a major ash-flow and caldera complex in the southern Andes of central Chile. *GSA Bull* 95:45–54
- 1124 Hoffmann JAJ (1975) Atlas climatico de America del Sur. World Meteorol Organ
- 1125 Huyer A, Knoll M, Paluszkiwicz T, Smith RL (1991) The Peru undercurrent—a study in variability. *Deep-Sea Res Part A-Oceanogr Res Papers* 38:S247–S271
- 1126 Jessen GL, Pantoja S, Gutiérrez MH, Quiñones RA, González RR, Sellanes J, Kellermann M, Hinrichs K-U (2011) Methane in shallow cold seeps at Mocha Island off central Chile. *Cont Shelf Res* 31:574–581. doi:510.1016/j.csr.2010.1012.1012
- 1127 Kastner M, Elderfield H, Martin JB (1991) Fluids in convergent margins—What do we know about their composition, origin, role in diagenesis and importance for oceanic chemical fluxes. *Philos Trans R Soc A* 335(1638):243–259
- 1128 Klauke I, Weinrebe W, Linke P, Kläschen D, Bialas J (2012) Sidescan sonar imagery of widespread fossil and active cold seeps along the central Chilean continental margin. *Geo-Marine Lett* 1–11. doi:10.1007/s00367-012-0283-1
- 1129 Kukowski N, Oncken O (2006) Subduction Erosion—the “Normal” mode of fore-arc material transfer along the Chilean Margin? In: Oncken O, Chong G, Franz G, Giese P, Götze H-J, Ramos VA, Strecker MR, Wigger P (eds) *The Andes-Active subduction Orogeny*. Springer, Berlin, pp 213–232
- 1130 Lamy F, Hebbeln D, Wefer G (1998) Terrigenous sediment supply along the Chilean continental margin: modern regional patterns of texture and composition. *Geol Rundsch* 87:477–494
- 1131 Lamy F, Hebbeln D, Wefer G (1999) High-resolution marine record of climatic change in mid-latitude Chile during the last 28,000 years based on terrigenous sediment parameters. *Quat Res* 51:83–93

- 1226 Lamy F, Hebbeln D, Rohl U, Wefer G (2001) Holocene rainfall
1227 variability in southern Chile: a marine record of latitudinal shifts
1228 of the Southern Westerlies. *Earth Planet Sci Lett* 185:369–382
1229 Lange D, Rietbrock A, Haberland C, Bataille K, Dahm T, Tillmann F,
1230 Flüß ER (2007) Seismicity and geometry of the South Chilean
1231 subduction zone (41.5°S–43.5°S): implications for controlling
1232 parameters. *Geophys Res Lett* 34:L06311. doi:10.1029/2006
1233 GL029190
- 1234 Laursen J, Normark WR (2002) Late Quaternary evolution of the San
1235 Antonio submarine canyon in the central Chile forearc (similar
1236 to 33 degrees S). *Marine Geol* 188:365–390
- 1237 Laursen J, Normark WR (2003) Impact of structural and autocyclic
1238 basin-floor topography on the depositional evolution of the deep-
1239 water Valparaiso forearc basin, central Chile. *Basin Res*
1240 15:201–226
- 1241 Laursen J, Scholl DW, von Huene R (2002) Neotectonic deformation
1242 of the central Chile margin: deepwater forearc basin formation in
1243 response to hot spot ridge and seamount subduction. *Tectonics*
1244 21:1038. doi:10.1029/2001TC901023
- 1245 Linke P (2011) RV SONNE CRUISE SO-210 - ChiFlux- Identifica-
1246 tion and investigation of fluid flux, mass wasting and sediments
1247 in the forearc of the central Chilean subduction zone. *Berichte*
1248 *aus dem Leibniz-Institut für Meereswissenschaften an der*
1249 *Christian-Albrechts-Universität zu Kiel* 44:1–107
- 1250 Lohrmann J, Kukowski N, Krawczyk CM, Oncken O, Sick C, Sobiesiak
1251 M, Rietbrock A (2006) Subduction channel evolution in Brittle
1252 Fore-Arc Wedges—a combined study with scaled sandbox
1253 experiments, seismological and reflection seismic data and
1254 geological field evidence. In: Oncken O, Chong G, Franz G,
1255 Giese P, Götze H-J, Ramos VA, Strecker MR, Wigger P (eds) *The*
1256 *Andes-Active subduction Orogeny*. Springer, Berlin, pp 237–262
- 1257 Lomnitz C (2004) Major earthquakes of Chile: a historical survey,
1258 1535–1960. *Seismol Res Lett* 75(3):368–378. doi:10.1785/gssrl.
1259 75.3.368
- 1260 López-Escobar L, Kilian R, Kempton PD, Tagiri M (1993) Petrog-
1261 raphy and geochemistry of quaternary rocks from the Southern
1262 Volcanic Zone of the Andes between 41° and 46°S, Chile. *Rev*
1263 *Geol Chile* 20(1):33–55
- 1264 Martin JB, Kastner M, Egeberg PK (1995), Origins of saline fluids at
1265 convergent margins. In: Taylor B, Natland JP (eds) *Active*
1266 *margins and marginal basins of the Western Pacific*, *Geophys.*
1267 *Monogr. Ser.*, vol 88. AGU, Washington, DC, pp 219–239
- 1268 Melnick D, Echtler HP (2006a) Inversion of forearc basins in south-
1269 central Chile caused by rapid glacial age trench fill. *Geology*
1270 34:709–712. doi:10.1130/G22440.22441
- 1271 Melnick D, Echtler HP (2006b) Morphotectonic and geologic digital
1272 map compilations of the south-central Andes (36°–42°S). In:
1273 Oncken O, Chong G, Franz G, Giese P, Götze HJ, Ramos M,
1274 Strecker MR, Wigger P (eds) *The Andes-Active subduction*
1275 *Orogeny*, vol 1. Springer, Berlin, pp 565–568
- 1276 Melnick D, Bookhagen B, Echtler HP, Strecker MR (2006) Coastal
1277 deformation and great subduction earthquakes, Isla Santa María,
1278 Chile (37°S). *GSA Bull* 118:1463–1480. doi:1410.1130/B25865.
1279 25861
- 1280 Melnick D, Bookhagen B, Strecker MR, Echtler HP (2009) Segmen-
1281 tation of megathrust rupture zones from fore-arc deformation
1282 patterns over hundreds to millions of years, Arauco peninsula,
1283 Chile. *J Geophys Res* 114:B01407. doi:01410.01029/02008JB
1284 005788
- 1285 Mix AC, Tiedemann R, Blum P, Shipboard P (2003) Initial reports,
1286 ODP-leg 202. *Proc. ODP, Init. Repts.*, 202 [Online]
- 1287 Montgomery DR, Balco G, Willett SD (2001) Climate, tectonics, and
1288 the morphology of the Andes. *Geology* 29:579–582
- 1289 Morales E (2003) Methane hydrates in the Chilean continental
1290 margin. *Electr J Biotechnol* 6(2):80–84
- Mordojoovic C (1974) Geology of a part of the Pacific margin of Chile.
In: Burk CA, Drake CL (eds) *The geology of continental*
1292 *margins*. Springer, New York, pp 591–598
1293 Mordojoovic C (1981) Sedimentary basins of Chilean Pacific offshore.
1294 In: *Energy resources of the Pazific region*, vol 12. American
1295 *Association of Petroleum Geologists*, pp 63–68
1296 Moreno MS, Bolte J, Klotz J, Melnick D (2009) Impact of megathrust
1297 geometry on inversion of coseismic slip from geodetic data:
1298 application to the 1960 Chile earthquake. *Geophys Res Lett*
1299 36:L16310. doi:16310.11029/12009GL039276
- Moscoco E, Grevemeyer I, Contreras-Reyes E, Flueh ER, Dzierma Y,
1301 Rabbel W, Thorwart M (2011) Revealing the deep structure and
1302 rupture plane of the 2010 Maule, Chile earthquake (Mw = 8.8)
1303 using wide angle seismic data. *Earth Planet Sci Lett*
1304 307:147–155. doi:110.1016/j.epsl.2011.1004.1025
- Muñoz P, Lange CB, Gutiérrez D, Hebbeln D, Salamanca MA,
1306 Dezileau L, Reyss JL, Benninger LK (2004) Recent sedimen-
1307 tation and mass accumulation rates based on 210Pb along the
1308 Peru-Chile continental margin. *Deep Sea Res* 51:2523–2541
1309 Naranjo JA, Stern CR (1998) Holocene explosive activity of Hudson
1310 Volcano, southern Andes. *Bull Volcanol* 59:291–306
- Naranjo JA, Stern CR (2004) Holocene tephrochronology of the
1312 southernmost part (42°30′–45°S) of the Andean Southern Vol-
1313 canic Zone. *Revista Geológica de Chile* 31:225–240
1314 Oliver PG, Sellanes J (2005) New species of Thyasiridae from a
1315 methane seepage area off Concepción, Chile. *Zootaxa* 1092:1–20
1316 Oncken O, Hindle D, Kley J, Elger K, Victor P, Schemmann K (2006)
1317 Deformation of the Central Andean upper plate system—facts,
1318 fiction, and constraints for plateau models. In: Oncken O, Chong
1319 G, Franz G, Giese P, Götze H-J, Ramos VA, Strecker MR,
1320 Wigger P (Eds.): *The Andes-Active subduction Orogeny*.
1321 Springer, Berlin. doi:10.1007/978-3-540-48684-8_1
- Pizarro O, Shaffer G, Dewitte B, Ramos M (2002) Dynamics of
1323 seasonal and interannual variability of the Peru-Chile Undercur-
1324 rent. *Geophys Res Lett* 29(12). doi:10.1029/2002GL014790
- Quiroga E, Sellanes J (2009) Growth and size-structure of *Stegophi-*
1326 *ura* sp. (Echinodermata: Ophiuroidea) on the continental slope
1327 off central Chile: a comparison between cold seep and non-seep
1328 sites. *J Marine Biol Assoc UK* 89:421–428. doi:10.1017/
1329 S0025315408002786
- Raitzsch M, Völker D, Heubeck C (2007) Neogene sedimentary and
1331 mass-wasting processes on the continental margin off south-
1332 central Chile inferred from dredge samples. *Marine Geol*
1333 244:166–183. doi:10.1016/j.margeo.2007.06.007
- Ranero CR, von Huene R, Weinrebe W, Reichert C (2006) Tectonic
1335 processes along the Chile convergent margin. In: Oncken O,
1336 Chong G, Franz PGG, Götze H-J, Ramos VA, Strecker MR,
1337 Wigger P (eds) *The Andes-Active subduction Orogeny*. *Frontiers*
1338 *in earth sciences*. Springer, Berlin, pp 91–123
1339 Rauch K (2005) Cyclicity of Peru-Chile trench sediments between 36
1340 degrees and 38 degrees S: a footprint of paleoclimatic varia-
1341 tions? *Geophys Res Lett* 32. doi:10.1029/2004GL022196
- Rehak K, Strecker MR, Echtler HP (2008) Morphotectonic segmen-
1343 tation of an active forearc, 37°–41°S, Chile. *Geomorphology*
1344 94:98–116. doi:110.1016/j.geomorph.2007.1005.1002
- Reichert C (2002) Cruise Report SO161, leg 2&3, SPOC, subduction
1346 processes off Chile. BGR internal report, pp 1–154
1347 Rodrigo C (2010) Cañones submarinos en el margen continental
1348 chileno. In: Díaz-Naveas J, Frutos J (2010). *Geología Marina de*
1349 *Chile*. Comité Oceanográfico Nacional de Chile—Pontificia
1350 *Universidad Católica de Valparaíso—Servicio Nacional de*
1351 *Geología y Minería de Chile* 32–35
- Rodrigo C, González-Fernández A, Vera E (2009) Variability of the
1353 bottom-simulating reflector (BSR) and its association with
1354 tectonic structures in the Chilean margin between Arauco Gulf
1355

- 1356 (37°S) and Valdivia (40°S). *Marine Geophys Res* 30:1–19. doi:
1357 [10.1007/s11001-11009-19064-11002](https://doi.org/10.1007/s11001-11009-19064-11002)
- 1358 Rosenau MR (2004) Tectonics of the southern Andean intra-arc zone
1359 (38°–42°S). PhD thesis, Freie Universität Berlin, pp 1–195
- 1360 Rosenau M, Melnick D, Echtler H (2006) Kinematic constraints on
1361 intra-arc shear and strain partitioning in the southern Andes
1362 between 38°S and 42°S latitude. *Tectonics* 25:TC4013. doi:
1363 [10.1029/2005TC001943](https://doi.org/10.1029/2005TC001943)
- 1364 Sahling H, Masson DG, Ranero CR, Hühnerbach V, Weinrebe W,
1365 Klauke I, Bürk D, Brückmann W, Suess E (2008) Fluid seepage
1366 at the continental margin offshore Costa Rica and southern
1367 Nicaragua. *Geochem Geophys Geosyst* 9(5):Q05S05. doi:
1368 [10.1029/2008GC001978](https://doi.org/10.1029/2008GC001978)
- 1369 Sánchez M (2004) Evolución tectónica de Isla Mocha [38 20' S, 73
1370 55' W]: configuración de un sistema anómalo en el margen
1371 occidental de la cuenca de antearco de Arauco. MSc thesis,
1372 Universidad de Concepción, Concepción, pp 1–108
- 1373 Scherwath M, Contreras-Reyes E, Flueh ER, Grevemeyer I, Kra-
1374 bbenhoeft A, Papenberg C, Petersen CJ, Weinrebe RW (2009)
1375 Deep lithospheric structures along the southern central Chile
1376 Margin from wide-angle P-wave modelling. *Geophys J Int*
1377 179:579–600. doi:[10.1111/j.1365-1246X.2009.04298.x](https://doi.org/10.1111/j.1365-1246X.2009.04298.x)
- 1378 Sellanes J, Krylova E (2005) A new species of Calyptogena (Bivalvia:
1379 Vesicomidae) from a recently discovered methane seepage area
1380 of Concepcion Bay, Chile (~36°S). *J Marine Biol Assoc UK*
1381 85(4):969–976
- 1382 Sellanes J, Quiroga E, Gallardo VA (2004) First direct evidences of
1383 methane seepage and associated chemosynthetic communities in
1384 the bathyal zone off Chile. *J Marine Biol Assoc UK* 84(5):1065–
1385 1066
- 1386 Sellanes J, Quiroga E, Neira C (2008) Megafauna community
1387 structure and trophic relationships at the recently discovered
1388 Concepcion Methane Seep Area, Chile, ~36°S. *ICES J Marine*
1389 *Sci J Conseil* 65:1102–1111
- 1390 Shaffer G, Salinas S, Pizarro O, Vega A, Hormanzabal S (1995)
1391 Currents in the deep ocean off Chile (30°S). *Deep Sea Res*
1392 42:425–436
- 1393 Shaffer G, Pizarro O, Djurfeldt L, Salinas S, Rutllant J (1997)
1394 Circulation and low-frequency variability near the Chilean coast:
1395 remotely forced fluctuations during the 1991–92 El Niño. *J Phys*
1396 *Oceanogr* 27:217–235
- 1397 Shaffer G, Hormazabal S, Pizarro O, Salinas S (1999) Seasonal and
1398 interannual variability of currents and temperature off central
1399 Chile. *J Geophys Res* 104:29951–29961
- 1400 Sick C, Yoon M-K, Rauch K, Buske S, Lüth S, Araneda M, Bataille
1401 K, Chong G, Giese P, Krawczyk C, Mechie J, Meyer H (2006)
1402 Seismic images of accretive and erosive subduction zones from
1403 the Chilean Margin. In: Oncken O, Chong G, Franz G, Giese P,
1404 Götze H-J, Ramos VA, Strecker MR, Wigger P (eds) *The Andes-*
1405 *Active subduction Orogeny*. Springer, Berlin, pp 147–171
- 1406 Siebert L, Simkin T (2002) *Volcanoes of the world: an illustrated*
1407 *catalog of holocene volcanoes and their eruptions*. Smithsonian
1408 *Institution. Global Volcanism Program Digital Information*
1409 *Series, GVP-3*, (<http://www.volcano.si.edu/world/>)
- 1410 Somoza R (1998) Updated Nazca (Farallon)-South America relative
1411 motions during the last 40 My: implications for mountain
1412 building in the central Andean region. *J S Am Earth Sci*
1413 11:211–215. doi:[10.1016/S0895-9811\(98\)00012-1](https://doi.org/10.1016/S0895-9811(98)00012-1)
- 1414 Sruoga P, Llambías EJ, Fauqué L, Schonwandt D, Repol DG (2005)
1415 Volcanological and geochemical evolution of the Diamante
1416 Caldera–Maipo volcano complex in the southern Andes of
1417 Argentina (34°10'S). *J S Am Earth Sci* 19:399–414
- 1418 Stern CR (2004) Active Andean volcanism: its geologic and tectonic
1419 setting. *Revista geológica de Chile* 31:161–206
- 1420 Stern CR, Moreno H, Lopez-Escobar L, Clavero JE, Lara LE, Naranjo
1421 JA, Parada MA, Skewes MA (2007) Chilean volcanoes. In:
Moreno T, Gibbons W (eds) *The geology of Chile*. Geological
Society of London, London, pp 147–178
- Strub T, Mesias J, Montecino V, Rutllant J, Salinas S (1998) Coastal
ocean circulation off western South America. Coastal segment.
In: Robinson A, K Brink (eds) *The Sea*, vol 11. Wiley, New
York, pp 273–313
- Stuardo J, Valdovinos C (1988) A new bathyal Calyptogena from the
coast of central Chile (Bivalvia: Vesicomidae). *Venus*
47:241–250
- Stuut J-BW, Kasten S, Lamy F, Hebbeln D (2007) Sources and modes
of terrigenous sediment input to the Chilean continental slope.
Quat Int Lacustrine Marine Arch Environ Variab Across S Am
161:67–76. doi:[10.1016/j.quaint.2006.1010.1041](https://doi.org/10.1016/j.quaint.2006.1010.1041)
- Thomson SN (2002) Late Cenozoic geomorphic and tectonic
evolution of the Patagonian Andes between latitudes 42 degrees
S and 46 degrees S; an appraisal based on fission-track results
from the transpressional intra-arc Liquiñe-Ofqui fault zone. *Geol*
Soc Am Bull 114:1159–1173
- Thornburg TM, Kulm LD, Hussong DM (1990) Submarine-fan
development in the Southern Chile trench—a dynamic interplay
of tectonics and sedimentation. *Geol Soc Am Bull* 102:1658–1680
- Treude T, Niggemann J, Kallmeyer J, Wintersteller P, Schubert CJ,
Boetius A, Jørgensen BB (2005) Anaerobic oxidation of
methane and sulfate reduction along the Chilean continental
margin. *Geochim Cosmochim Acta* 69:2767–2779
- Vargas G, Fariás M, Carretier S, Tassara A, Baize S, Melnick D (2011)
Coastal uplift and tsunami effects associated to the 2010 Mw 8.8
Maule earthquake in Central Chile. *Andean Geol* 38:219–238
- Völker D, Wiedicke M, Ladage S, Gaedicke C, Reichert C, Rauch K,
Kramer W, Heubeck C (2006) Latitudinal variation in sedimentary
processes in the Peru–Chile trench off central Chile. In:
Oncken O, Chong G, Franz G, Giese P, Götze H-J, Ramos VA,
Strecker MR, Wigger P (eds) *The Andes-Active subduction*
Orogeny. Springer, Berlin, pp 193–216
- Völker D, Reichel T, Wiedicke M, Heubeck C (2008) Turbidities
deposited on Southern Central Chilean seamounts: evidence for
energetic turbidity currents. *Marine Geol* 251:15–31
- Völker D, Weinrebe W, Behrmann JH, Bialas J, Klaeschen D (2009)
Mass wasting at the base of the south central Chilean continental
margin: the Reloca Slide. *Adv Geosci* 22:155–167
- Völker D, Scholz F, Geersen J (2011) Analysis of submarine
landsliding in the rupture area of the 27 February 2010 Maule
earthquake, Central Chile. *Marine Geol* 288:79–89. doi:[10.1016/
j.margeo.2011.08.003](https://doi.org/10.1016/j.margeo.2011.08.003)
- Völker D, Geersen J, Weinrebe W, Behrmann J (2012) Submarine
mass wasting off Southern Central Chile: distribution and
possible mechanisms of slope failure at an active continental
margin. In: Yamada Y, Kawamura K, Ikehara K, Ogawa Y,
Urgeles R, Mosher D, Chaytor JD, Strasser M (Eds) *Submarine*
mass movements and their consequences V, pp 379–390
- von Huene R, Corvalan J, Flueh ER, Hinz K, Korstgard J, Ranero CR,
Weinrebe RW, Klaeschen D, Naveas JLD, Harms G, Spiegler D,
Biebow N, Locker S, Kruger D, Morales E, Vergara H, Yanez G,
Valenzuela E, Wall R, Trinhammer P, Laursen J, Scholl D, Kay
S, Dominguez S, Segl M, Beese D, Lamy F, Bialas J, Biegling A,
Gerdom M, Hojka AM, Hoppenworth R, Husem S, Krastel S,
Kulowski N, Morawe MP, Muñoz AED, Lefmann AK, Vidal
NM, Zelt C, Hinz K, Block M, Damm V, Fritsch J, Neben S,
Reichert C, Schreckenberger B (1997) Tectonic control of the
subducting Juan Fernandez Ridge on the Andean margin near
Valparaiso, Chile. *Tectonics* 16:474–488
- Wang K, Hu Y, Bewis M, Kendrick E, Smalley R, Vargas RB, Lauria
E (2007) Crustal motion in the zone of the 1960 Chile
earthquake: detangling earthquake-cycle deformation and fore-
arc-sliver translation. *Geochem Geophys Geosyst* 8:Q10010.
doi:[10.1029/2007GC001721](https://doi.org/10.1029/2007GC001721)

- 1488 Weinrebe W, Schenk S (2006) FS Meteor Fahrtbericht/Cruise Report
 1489 M67/1 CHILE-MARGIN-SURVEY Talcahuano (Chile)—
 1490 Balboa (Panama) 20.02.-13.03.2006. Berichte aus dem
 1491 Leibniz-Institut für Meereswissenschaften an der Christian-
 1492 Albrechts-Universität zu Kiel, 07:1–112. doi:[10.3289/ifm-
 1493 geomar_rep_7_2006](https://doi.org/10.3289/ifm-geomar_rep_7_2006)
- 1494 Weinrebe W, Flueh E, Hasert M, Behrmann J, Völker D, Geersen J,
 1495 Ranero C, Diaz-Naveas J (2011). 16 years, 16 cruises, 1.6 billion
 1496 soundings: a compilation of high-resolution multibeam Bathym-
 1497 etry of the active plate boundary along the Chilean Continental
 1498 Margin. Abstract OS24A-06 presented at AGU Fall Meeting
 1499 2011, San Francisco, CA
- 1500 Wiedicke-Hombach M (2002) Fahrtbericht SO161-5 SPOC (Subduc-
 1501 tion Processes off Chile) BGR Hannover 1–120
- Willner AP (2005) Pressure-temperature evolution of a Late Palaeo-
 zoic paired metamorphic belt in north-central Chile (34
 degrees-35 degrees 30' S). *J Petrol* 46:1805–1833
- Willner AP, Thomson SN, Kröner A, Wartho JA, Wijbrans JR, Hervé
 F (2005) Time markers for the evolution and exhumation history
 of a Late Palaeozoic paired metamorphic belt in north-central
 Chile (34°–35°30'S). *J Petrol* 46:1835–1858
- Scholz F, Hensen C, Schmidt M, Geersen J (submitted) Organic
 matter cycling, submarine weathering and subduction dewater-
 ing across the central Chilean forearc (~36°S). *Geochem
 Geophys Geosyst* (Submitted to)
- Zapata RA (2001) Estudio batimétrico del margen chileno. Master
 thesis, Universidad de Chile, Santiago de Chile, pp 1–113

UNCORRECTED PROOF